

AMERICAN UNIVERSITY OF BEIRUT

ESTABLISHING A PERTINENT IN VITRO MODEL
OF THE BLOOD BRAIN BARRIER TO ELUCIDATE
THE MECHANISMS OF INVASION AND DRUG
PERMEABILITY TO THE BRAIN

by
FATIMA FOUAD BALLOUT

A thesis
submitted in partial fulfillment of the requirements
for the degree of Master of Science
to the Department of Anatomy, Cell Biology and Physiological Sciences
of the Faculty of Medicine
at the American University of Beirut

Beirut, Lebanon
August 2023

AMERICAN UNIVERSITY OF BEIRUT

ESTABLISHING A PERTINENT IN VITRO MODEL OF THE
BLOOD BRAIN BARRIER TO ELUCIDATE THE MECHANISMS
OF INVASION AND DRUG PERMEABILITY TO THE BRAIN

by
FATIMA FOUAD BALLOUT

Approved by:



Dr. Marwan El-Sabban, Professor
Department of Anatomy, Cell Biology and Physiological Sciences

Advisor



Dr. Hiba El-Hajj, Associate Professor
Department of Experimental Pathology, Immunology and Microbiology

Co-Advisor



Dr. Wassim Abou-Kheir, Associate Professor
Department of Anatomy, Cell Biology and Physiological Sciences

Member of Committee



Dr. Georges Daoud, Associate Professor
Department of Anatomy, Cell Biology and Physiological Sciences

Member of Committee

Date of thesis defense: August 31st, 2023

AMERICAN UNIVERSITY OF BEIRUT

THESIS RELEASE FORM

Student Name: Ballout Fatima Fouad
Last First Middle

I authorize the American University of Beirut, to: (a) reproduce hard or electronic copies of my thesis; (b) include such copies in the archives and digital repositories of the University; and (c) make freely available such copies to third parties for research or educational purposes:

- As of the date of submission
- One year from the date of submission of my thesis.
- Two years from the date of submission of my thesis.
- Three years from the date of submission of my thesis.



Signature

04/09/2023

ACKNOWLEDGEMENTS

Thank you God for placing my footsteps on the path to pursue knowledge because as I walk one step further, I realize how little do I know and how much there is. Yet, while the entire universe is enfolded within us, there is no need to look beyond as what we seek is with us if only we reflect...

I am fortunate to be part of such peculiar family and friends. No words can describe my gratitude to baba and mama, Fouad and Wafaa, for being my parents, friends and support system.

I am extremely grateful to Dr. Marwan El-Sabban for being there. I am lucky to have an exceptional mentor as you. Not only did you teach me science but also life. Thank you for all your perpetual guidance.

I am delighted to join MES family for this stage in my life. Every single one was more than helpful. Special thanks to my brother and partner (actually teacher), Mario, who made the worst times bearable and fruitful.

Finally, I offer my sincere appreciation for the learning opportunities provided by my committee members: Co-advisor Dr. Hiba El-Hajj, Dr. Wassim Abou-Kheir and Dr. Georges Daoud.

Thank you all!

ABSTRACT OF THE THESIS OF

Fatima Fouad Ballout

for

Master of Science

Major: Neuroscience

Title: Establishing a Pertinent In vitro model of the Blood Brain Barrier to Elucidate Mechanisms of Invasion and Drug Permeability to the Brain

The maintenance of homeostasis in the brain relies on the restrictive permeability of the blood brain barrier (BBB). Neurological disorders, neurodegeneration, infectious insults, and tumor metastasis to the brain are all consequences of the loss of structural integrity of the BBB. Specific to Lebanon, 80% of the Lebanese population is thought to be infected with *Toxoplasma gondii* (*T. gondii*). Chronic toxoplasmosis (CT) is established after the parasite crosses the BBB to form cysts in the brain. The latter is associated with primary neuropathies, neuropsychiatric and behavioral disorders as well as brain cancers. Furthermore, 1 in 8 women will develop breast cancer in their lifetime. One of the most devastating consequences of breast cancer development and progression is secondary metastasis to the brain. Hence, it is imperative to find a relevant way to study the BBB to curb the deleterious side effects of it being breached. Current models fail to recapitulate the fundamental properties required to mirror the pathophysiological features of the BBB, leaving a gap in the application and translation of the research for medical application. Therefore, there is a need for effective modeling of the BBB to elucidate mechanisms of a variety of diseases including parasitic infection, metastasis of cancer to the brain, and to assess current drugs for BBB permeability and for novel drug screening. In this study, we developed a three-dimensional (3D) model that recapitulates the physiological and molecular properties of the BBB *in vitro*. This was achieved using a trans-well, cell-cell and cell-matrix interaction model. This model uniquely uses primary human endothelial cells and astrocytes, as well as subendothelial basement membrane to faithfully mimic the cyto-architecture of the BBB. Barrier permeability was then assessed using trans epithelial/ endothelial electrical resistance (TEER) and a variety of permeability tracers. We used this model as a platform to assess the invasion of *Toxoplasma gondii* (*T. gondii*) to the brain and breast cancer metastasis. This novel BBB model will contribute to the assessment of known drugs that are BBB permeable as well as discovering novel drugs that can be delivered to the brain. In doing so, we hope to extricate the molecular mechanisms of these breaches of the BBB to contribute to the amelioration of the outcomes of diagnoses of *T. gondii* infection or metastatic breast cancer.

Keywords: Blood brain barrier, parasitic infection, breast cancer metastasis

TABLE OF CONTENTS

ACKNOWLEDGEMENTS	1
ABSTRACT	2
ILLUSTRATIONS	6
TABLES	7
ABBREVIATIONS	8
INTRODUCTION	9
1.1. Blood brain barrier concept and constituents:	9
1.1.1. Cellular components of BBB:.....	10
1.1.2. Basement membrane:.....	13
1.1.3. Functions of BBB:	13
1.1.4. Major transport pathways of different molecules through the BBB:.....	14
1.1.5. Restricted drug permeability to the brain:	16
1.2. Disruption of the permeability of the blood brain barrier:.....	16
1.2.1. Cancer metastasis: BBB cellular infiltration	17
1.2.2. Toxoplasma Gondii translocation into the brain:	21
1.3. In vitro models that mimic the blood brain barrier:	26
AIMS & OBJECTIVE OF THE STUDY	30
MATERIALS AND METHODS	31
3.1. Cell lines and culture conditions.....	31
3.1.1. ECV-304 cell line:	31

3.1.2. Human Aortic Endothelial Cells (HAEC):	31
3.1.3. Normal Human Astrocytes (NHA):	32
3.1.4. MDA-MB231 cell line:.....	33
3.2. Cell viability and growth assay.....	34
3.3. BBB modeling:	35
3.3.1. Coculture of HAEC and NHA:	35
3.4. Evaluation of the barrier integrity:.....	37
3.4.1. Transepithelial/transendothelial electrical resistance (TEER):.....	37
3.4.2. Permeability assay:	37
3.5. Molecular analysis of junctional proteins expression:.....	39
3.5.1. Gene expression assessment by Quantitative Real-Time Polymerase Chain Reaction:.....	39
3.5.2. Immunofluorescence for phenotypic characterization and adherent junctional protein localization:	41
3.6. MDA-MB 231 cells extravasation assay:	42
3.6.1. Immunofluorescence for migratory BC cells:	43
3.7. <i>T. gondii</i> invasion assay:.....	44
3.7.1. Parasitic infection of the BBB model:	44
3.7.2. Immunofluorescence for invading parasites/infected monocytes:.....	45
RESULTS	46
4.1. Endothelial monolayer optimization using ECV-304 cells:	46
4.2. Endothelial monolayer modelling using HAEC:	48
4.3. Normal Human Astrocyte maintenance and 3D culture:.....	50
4.4. BBB modeling using HAEC and NHA:	52
4.5. MDA-MB231 cell lines successfully extravasate endothelial monolayers: ...	54

4.5.1.	Extravasation through ECV-304 monolayer:	54
4.5.2.	Extravasation through HAEC monolayer:	56
4.5.3.	Extravasation through HAEC and NHA coculture:.....	58
4.6.	<i>T. gondii</i> auspiciously disseminate into endothelial monolayers:	59
DISCUSSION & CONCLUSION		60
REFERENCES		62

ILLUSTRATIONS

Figure

1. Schematic presentation of a cross section of the blood brain barrier (BBB) (done by BioRender).....	10
2. Schematic diagram of the transport mechanisms across the BBB through paracellular and transcellular pathway (done by BioRender).....	15
3. Schematic diagram of the metastasis of cancer cells across the BBB through paracellular and transcellular pathways ((Fares et al., 2020):	21
4. Modalities of infection (Hill & Dubey, 2016).	22
5. Scenarios of modes of entry of <i>T. gondii</i> into the brain	26
6. pGFP-V-RS vector used to transfect MDA-MB231 by shCx 43(GFP: green fluorescent protein).	34
7. A. Timeline of the stages of model establishment B. HAEC and NHA coculture and further barrier integrity assessment assay done by BioRender.	36
8. Flow chart of the different insert groups and subsequent division of BC extravasation assay.	43
9. Flow chart of the different insert groups and subsequent division of parasite invasion assay.	45
10. Endothelial monolayer optimization.....	47
11. HAEC monolayer characterization.	49
12. Characterization of NHA morphology, proliferation, and cell viability.....	51
13. BBB modelling using HAEC and NHA and barrier integrity evaluation.....	53
14. MDA-MB231 cell lines extravasation through ECV-304 monolayer.	55
15. MDA-MB231 cell lines extravasation through HAEC monolayer.	57
16. MDA-MB231 cell lines extravasation through HAEC and NHA coculture.	58
17. Infection of HAEC cells of the monolayer by GFP labelled tachyzoite II.	59

TABLES

Table

1. Different models of the blood brain barrier (Ferro et al., 2020; Saliba et al., 2018; Sivandzade & Cucullo, 2018; Stone et al., 2019).....	29
2. Seeding density of different cell lines per cm ²	35
3. RT-qPCR primer sequences and annealing temperatures for studied human genes	41
4. Antibodies used for immunofluorescence	42

ABBREVIATIONS

BBB	Blood brain barrier
CNS	Central nervous system
NVU	Neurovascular unit
EC	Endothelial cells
Tjs	Tight junctions
ECM	Extracellular matrix
JAMs	Junctional adhesion molecules
EMT	Epithelial-to-mesenchymal transition
MET	Mesenchymal-to-epithelial transition
BC	Breast cancer
BM	Brain metastasis
Cx 43	Connexion 43
E-cad	Epithelial cadherin
ZO-1	Zona occluden 1
CLDN 5	Claudin 5
<i>T. gondii</i>	Toxoplasma gondii
AT	Acute toxoplasmosis
CT	Chronic toxoplasmosis

CHAPTER 1

INTRODUCTION

1.1. Blood brain barrier concept and constituents:

The brain is the most complex and multifaceted organ of the human body (Rasmussen et al., 2022). It processes sensory input, computes decisions, and coordinates behavioral output (Nowinski, 2021). The brain is a three-pound organ lying in its bony shell and protected by cellular barriers that regulate and limit the molecular and cellular exchange between the blood and the brain parenchyma (Abbott et al., 2006; Coureuil et al., 2017).

Three main barrier systems contribute to the bioavailability of drugs, translocation of immune cells and the protection of the brain parenchyma from blood-borne external insults: the meningeal barrier, the blood cerebrospinal fluid barrier and the blood brain barrier (BBB) (Modarres et al., 2018; Olivera et al., 2021; Ross et al., 2021). The latter is the largest barrier in the central nervous system (CNS) (Ross et al., 2022).

The blood brain barrier is a dynamic interface that separates the peripheral blood flow from the brain parenchyma (Gosselet et al., 2021). The BBB is the central component of the neurovascular unit (NVU) which mainly consists of highly packed monolayer of fenestrated brain microvascular endothelial cells lying on the basement membrane and supported by pericytes and astrocytes end-feet (Arvanitis et al., 2020; Daneman & Prat, 2015; Modarres et al., 2018). (see Figure 1)

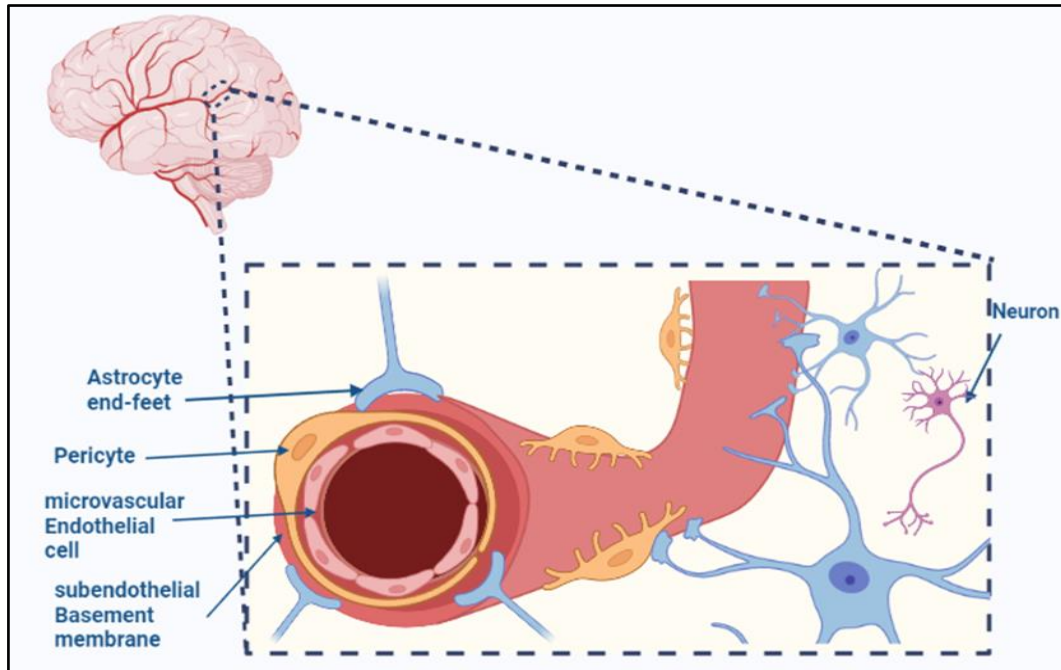


Figure 1: Schematic presentation of a cross section of the blood brain barrier (BBB) (done by BioRender).

1.1.1. Cellular components of BBB:

1.1.1.1. Brain microvascular endothelial cells:

The BBB endothelial cells (EC) are simple squamous epithelial cells that line the blood vessels but are quite different from other non-brain vascular endothelial cells (Daneman & Prat, 2015; Jamieson et al., 2017). They lack fenestrae, have high mitochondrial activity, exhibit abundant transporters and receptors required for selective recruitment of molecules and efflux of metabolites, and adjacent cells are firmly packed together by tight junctions (Tjs), including claudins, occludins, etc...(Hashimoto et al., 2023) Thus, these cells have low paracellular permeability (Sivandzade & Cucullo, 2018). They also express less leukocyte adhesion molecules the other microvascular EC (Galea, 2021). EC possess a variety of substrate transport systems that control the influx of polar nutrients into the brain, such as the superfamily of solute carriers (SLC family) for glucose and amino acid uptake (Cecchelli et al., 2007). They also have efflux pumps for

potential toxic substances or small lipophilic molecules ejected back into the circulation via ATP-binding cassette (ABC) superfamily, multi-drug resistant associated protein (MRPs), P-glycoprotein, etc...(Cecchelli et al., 2007; Galea, 2021) Moreover, the hemodynamic forces including shear stress (approximately $5-20 \text{ dyne.cm}^{-2}$ in capillaries) associated with blood flow induce change in many important characteristics of EC with influence on the expression of genes that intervene in morphology, proliferation, and inflammation (Cucullo et al., 2011; Wong et al., 2013).

1.1.1.2. Astrocytes:

Astrocytes represent the most abundant glial cells in the CNS and show different morphologies according to its location and association with other cells (Abbott et al., 2006; Verkman, 2002). At the NVU, astrocyte end-feet ensheath the vasculature at a ratio of single astrocyte to an average of 5 different blood vessels (1:5) (Halassa et al., 2007). Recent literature has stressed on the role of these end-feet as key checkpoints of the brain metabolism (Galea, 2021). For example, astrocyte end-feet express high density of orthogonal arrays of particles having water channel aquaporin 4 (AQP-4) which is a potassium channel involved in ion and volume regulation (Jackson et al., 2022; Verkman, 2002). Lately, literature has shown that the density of these channels decreases as the contact between astrocytic end-feet and the basement membrane is lost (Galea, 2021). Studies have strongly emphasized that astrocytes also play multiple roles that upregulate many BBB features resulting in a stronger physical barrier (Michinaga & Koyama, 2021). It has been established that astrocytic end-feet contribute to the increase of the expression of agrin, a heparin sulphate proteoglycan anchored at the basement membrane, that is important for the tightening and integrity of the BBB (Jackson et al., 2022; Verkman,

2002). In addition, further synergistic functions with other cell types are present (Abbott et al., 2006). For instance, astrocytes secrete a range of factors of which is angiotensin II that affects the expression and localization of the TJ5 zona occluden-1 present in endothelial cells (EC) resulting in a decrease of the BBB permeability (Heithoff et al., 2021). Similarly, it facilitates strong connexin-mediated gap junctions (GJs) adhesion to EC thus maintaining the barrier's integrity (Boulay et al., 2016; Kim et al., 2016). Moreover, studies have further showed that astrocytes upregulate protease inhibitors activity against the activity of the degradative enzymes secreted by infiltration of lymphocytes (Pan et al., 2021).

1.1.1.3. Pericytes:

Vascular mural cells are referred to as vascular smooth muscle cells and pericytes (Mäe et al., 2021). While vascular smooth muscle cells surround arteries and veins, pericytes are embedded in the basement membrane of blood capillaries which show their contribution in the architecture, maintenance, contractility and generation of new blood vessels, where around 70-80% of the surface area of the capillaries is covered with pericytes' processes (Mäe et al., 2021; Uemura et al., 2020). Moreover, pericytes play a variety of functions that ensure the BBB integrity and contribute to its semi permeability such as regulating the entry of immune cells to the brain parenchyma, controlling protein expression and alignment of tight junctions in EC, and interfering in the pinocytosis activity across the BBB (Armulik et al., 2010; Rudziak et al., 2019).

1.1.2. Basement membrane:

The basement membrane is the noncellular component of the NVU and is a unique form of the extracellular matrix (ECM) found underneath the EC (Baeten & Akassoglou, 2011). It is a protein layer with a thickness of 50-100 nm and consisting of four major ECM proteins: laminin, collagen IV, perlecan and nidogen, which are synthesized predominantly by the cellular component of the BBB (Xu et al., 2019). However, the basement membrane's composition varies, particularly that of laminin isoforms, along the length of the postcapillary venules (least resistance part of the BBB) (Song et al., 2017). Studies have shown that mutations affecting the expression of laminin have resulted in detachment of glial cells from the basement membrane due to the loss of its integrity leading to defects of neuronal cell migration and layer formation (Yurchenco, 2011). Even though most studies focus on the cellular compartment of the blood brain barrier and its role in the restrictive permeability, some studies have shown that the basement membrane plays a protective role against disruptive physical stress, an anchor site for signaling events and a barrier for external chemicals and cells in the circulation, thus having a significant function in BBB integrity (Alahmari, 2021; Yurchenco, 2011).

1.1.3. Functions of BBB:

The major role of the blood brain barrier is to maintain the brain's homeostasis, and that is by moderating the barrier's permeability through controlling the access and efflux of different materials (Alyautdin et al., 2014). Consequently, it regulates molecular traffic, transports essential nutrients for neural cells' metabolism, and provides protection against xenobiotics and pathogens (Gosselet et al., 2021). Therefore, unlike the permeability through the blood vessels elsewhere, the communication between the extracellular

compartment and the brain parenchyma is restricted expelling troubling occurrences from happening and avoiding leakage (Kadry et al., 2020; Rasmussen et al., 2022). Hence, disrupting the integrity of the BBB is a critical and difficult point accompanied with the rise of detrimental and fatal situations.

1.1.4. Major transport pathways of different molecules through the BBB:

Highly regulated transport of different molecules across the BBB generally follows two major routes: paracellular and transcellular (Barar et al., 2016). Through the paracellular route, molecules, generally smaller than 70kDa, pass through the small gaps between neighboring endothelial cells due to the low permeability of the BBB (Hajal et al., 2021). The transmembrane proteins that are mainly responsible for the regulation of the transport through this route are the endothelial cells' tight junctions (Tjs). The primary Tjs identified at the BBB are the claudin family, especially claudin-5, and occludins like zonula occluden-1, junctional adhesion molecules (JAMs) and other adhesion junctions like vascular endothelial-cadherins...(Günzel & Yu, 2013). Claudins play the major role in the tightening of the BBB for more restricted permeability of small molecules <800 Da (Winkler et al., 2021). Moreover, occludins emphasize the tightening of the barrier by assuring its stability through interacting with the cell's cytoskeleton via scaffolding proteins, also acting as a sensor and protector facing insults such as hypoxia (Bellmann et al., 2014; Keep et al., 2018). However, transcellular transport which is across endothelial cells is divided into several modes depending on the size and chemical composition of the solute (Hajal et al., 2021). The first mode is the passive diffusion of gases like oxygen, ions and small lipophilic molecules through the lipid bilayer of the endothelial cells (Banks, 2009). Whereas large lipophilic substances that cannot diffuse

through the BBB, like cholesterol, are actively transported by the energy dependent ATP-binding cassette superfamily (ABC) transporter efflux, such as ABCB1 or P-glycoprotein (Abbott et al., 2010). In addition, specific solutes like glucose, neurotransmitters and different amino acids rely on active transportation via carrier mediated transporters present on the membrane of the endothelial cells (EC) (Zaragoza, 2020). Another mode is transcytosis that is partitioned into a specific transport mediated by the binding of the macromolecule to the relative membrane receptor and formation of a caveolae for the macromolecule to be engulfed into the cell, and another nonspecific transport of solutes that are ‘absorbed’ after electrostatically interacting with the cell’s surface (Tashima, 2020) (see Figure 2).

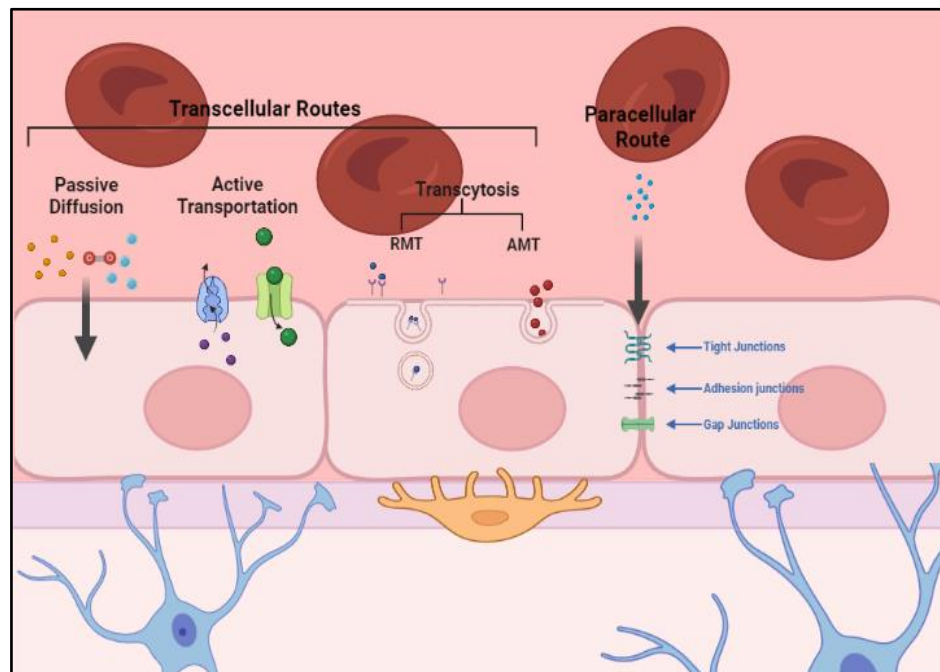


Figure 2: Schematic diagram of the transport mechanisms across the BBB through paracellular and transcellular pathway (done by BioRender). Small molecules (<70 kDa) pass between adjacent endothelial cells paracellularly. While other molecules are transported through the transcellular route... Ions, gases, and small lipophilic molecules rapidly diffuse through the cells. Larger lipophilic molecules and nutrients rely on active transportation, in addition to transcytosis that divides into specific receptor mediated transcytosis and nonspecific absorptive mediated transcytosis.

1.1.5. Restricted drug permeability to the brain:

The BBB hinders different molecules including treatments and drugs targeting the brain (such as statins, antidepressants, antitumor and others) from entering it: studies showed that up to 98% of drugs don't penetrate through BBB (Alyautdin et al., 2014). So, different approaches to enhance drug delivery were conceived, from which were direct intracerebral injection or co-administration of a hyperosmolar mannitol with the drug (Alyautdin et al., 2014; Brown et al., 2004; Wu et al., 2017). However, these approaches disrupted the blood brain barrier, caused damage to the brain tissue, and possessed risks for irreversible damage to the barrier's permeability (Kim et al., 2015).

Therefore, there is a need for effective modeling of the BBB to study its selectivity and functionality and to elucidate mechanisms of invasion of a variety of diseases and drug permeability to the brain.

1.2. Disruption of the permeability of the blood brain barrier:

The BBB is pivotal to maintain the homeostasis of the brain microenvironment. Its disruption is reported as a primary impact of aging, tissue damage, inflammation, edema, and neural dysfunction, and it has been recently marked as a long-lasting effect in neurodegeneration or other comorbidities like Alzheimer's disease and epilepsy...(Cash & Theus, 2020). Assessment of the disruption doesn't only include the structural and molecular profile of the barrier, like obtaining a 'leaky' barrier, but also include changes in various signaling pathways (Dulken et al., 2019). For example, the detection of interleukin-1beta (IL-1beta) by endothelial cells upon inflammation leads to the synthesis of prostaglandin E2 that diffuses into the brain parenchyma and act upon neurons and glial cells, thus inducing sickness behavior and enhancing cellular traffic especially

leukocytes infiltration into the brain due to the upregulation of certain adhesion proteins like integrins...(Dulken et al., 2019; Wilhelms et al., 2014).

Therefore, mild and transient changes in the permeability of the membrane was demonstrated as consequence to the disruption of the BBB either by infection or inflammation; however, the mechanism of entry and disruption is yet to be fully understood. Thus, incorporating this search in the *in-vitro* models facilitate the monitoring of these pathways to comprehend them.

1.2.1. Cancer metastasis: BBB cellular infiltration

Cancer is an intricate disease in which tumor cells are heterogeneous and interact with the surrounding extracellular matrix (ECM) and stromal cells that act as key determinants in tumor progression and therapeutics (Hao et al., 2019). As cancer is a leading cause of death worldwide accounting for nearly 10 million deaths in 2020, research has shown that metastasis is the principal cause of cancer-related deaths (Ganesh & Massagué, 2021).

1.2.1.1. Metastasis:

Cancer metastasis is a systematic disease involving the dissemination of tumor cells from the primary tumor site to undergo several cellular mechanisms to reach distal organs becoming secondary tumor sites (Suhail et al., 2019).

Studies have demonstrated the transition of tumor cells through a cascade of events to reach the secondary tumor site (Jolly et al., 2017). First, tumor cells undergo a process termed, epithelial-to-mesenchymal transition (EMT), where cells lose their epithelial phenotype (polarity and tight cell-cell adhesion) and gain mesenchymal traits of

invasiveness and motility (Savagner, 2015). However, this event is not only a cell-dependent one rather it can be influenced by the surrounding tissue microenvironment (Suhail et al., 2019). As for that, the insufficient supply to the cells as well as the oxygen tension fluctuation at this site leads to the activation of hypoxia-inducible factor (HIF) the latter can trigger EMT switch in tumor cells promoting a metastatic phenotype with the expression of various angiogenic factors including vascular endothelial growth factor (VEGF) (Lehmann et al., 2017). Second, these tumor cells show various changes in three prominent adhesion biomarkers (which are epithelial-cadherin, vimentin, and neural-cadherin), leading to their detachment from their surrounding matrix subsequently acquiring invasive properties (Tsai & Yang, 2013). Now, for their intravasation into the blood circulation, modified cancer cells enrich their secretory profile with matrix metalloproteases (MMPs) essential in the remodeling, degradation of the ECM and retraction of endothelial cells (Clark & Vignjevic, 2015). Upon reaching the surrounding circulation and due to anoikis, shear stress generated by blood flow, and scavenging of immune cells, not all circulating tumor cells (CTCs) are capable of survival (Wang et al., 2021). Upon arrival of the surviving CTCs to the target sites, tumor cells undergo a reverse process of mesenchymal-epithelial transition (MET) for the initiation of metastatic colonization (Ocaña et al., 2012). Thus, these cells will recognize organ specific adhesion molecules expressed on the surface of endothelial cells as the “seed and soil” theory by Stephan Paget states, and involve other cell adhesion molecules like integrins, vascular adhesion molecules and activated leukocyte cell adhesion molecules that reinforce cellular adhesion to neighboring endothelial cells (Fokas et al., 2007; Soto et al., 2014). Finally, the extravasation of tumor cells through endothelial cells’ basement membrane could be mediated by the secretion of VEGF, MMPs and other factors capable

of inducing dysregulation in the expression of Tj's and adhesion molecules thus permit the tumor cell to squeeze itself paracellularly (Friedl & Alexander, 2011; Yang et al., 2007). Besides endothelial cells at the secondary tumor site, additional cell types are also involved in the mechanism of extravasation (Wang et al., 2021). For example, to facilitate the transmigration of tumor cells, T lymphocytes secrete interferons that upregulate the expression of guanylate-binding protein 1 on endothelial cells (Mustafa et al., 2018). (see Figure 3).

1.2.1.2. Breast cancer (BC) metastasis to the brain:

In 2020, the world health organization (WHO) reported that breast cancer (BC) displayed as the most common cancer cases in the world (~2.26 million cases). BC is a highly miscellaneous disease possessing multiple subtypes which the 2013 St Gallen International Breast Cancer Conference defined them as: luminal A (ER/PR+, HER2-, KI67+), luminal B (ER/PR+, HER2-, KI67+), HER2+ B2 (ER/PR+, HER2 overexpression), HER2 overexpression (ER-,PR-, HER2 overexpression), basal-like triple-negative breast cancer (ER-, PR-, HER2-), and most recently molecular apocrine breast cancer (ER-, AR+) (Goldhirsch et al., 2013; Vranic & Gatalica, 2022).

Statistically, breast cancer accounts for approximately 20% among cancers that develop metastases involving the brain (Achrol et al., 2019; Duan et al., 2020). Unfortunately, the median survival time for BC patients decreases after brain metastasis (BM) to become 4-6 months (Brufsky et al., 2011).

For breast cancer to metastasize and reach the brain parenchyma, it undergoes the previously described cascade of events. However, studies have shown multiple key players involved in this cascade favoring metastasis to the brain. For example, several

investigations have shown that the decrease in connexin 43 (Cx 43) expression in breast cancer cells favors its mesenchymal phenotype with its associated invasive and metastatic properties; conversely Cx 43 upregulation orchestrates the MET by increasing the protein levels of epithelial markers such as E-cadherin (E-cad) and Zona occluden (ZO-1) (Kazan et al., 2019). Moreover, some mediators are regarded as specific ones that favor metastasis towards the brain rather than to any other organ by enhancing the ability of BC cells penetration through BBB like α 2,6-sialytransferase (ST6GALNAC5) that is expressed on BC cells and interact with EC cadherins (Bos et al., 2009). In addition, E-selectin expressed on EC of the BBB is induced by tumour necrosis factor α (TNF α), that is present at elevated levels in brain metastases (Geng et al., 2012). E-selectin will either bind to transmembrane glycoprotein CD44 on BC cells or to intercellular adhesion molecule (ICAM)-1 (Geng et al., 2012; Kang et al., 2015). The extravasation of BC through the blood brain barrier is not completely unraveled. It could be by disrupting the Tj's and adhesion molecules of the barrier's endothelial cells through several secretions: this would allow BC hustle to the brain's parenchyma or by increasing the permeability of BBB through transforming it to a permeable blood-tumor barrier (BTB) via vascular remodeling of pre-existing brain vessels, downregulation of basement membrane proteins, and affecting the phenotype of pericytes (Friedl & Alexander, 2011; Lockman et al., 2010; Pedrosa et al., 2018; Yang et al., 2007). Nonetheless, the exact mechanism of entry of these tumor cells and their role and interactions when encountering the NVU (basement membrane, pericytes and astrocytes' end-feet) remains under investigation.

As mentioned previously, most targeted agents and traditional chemotherapy treatments for BC or any other cancer have poor penetration through the blood brain barrier (Soffietti et al., 2020). Moreover, in the case of BCBM, local treatments including

surgery and even drugs showed limited therapeutic effect with challenges when encountering the BBB (Pellerino et al., 2020).

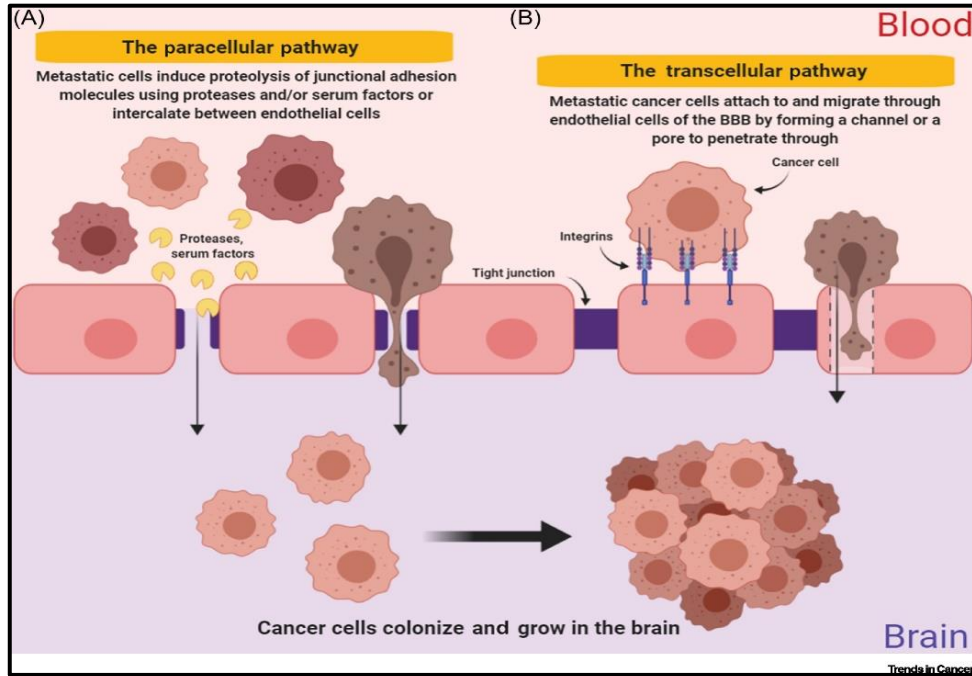


Figure 3: Schematic diagram of the metastasis of cancer cells across the BBB through paracellular and transcellular pathways ((Fares et al., 2020):

A. Extravasation of metastatic cancer cells through paracellular route between EC by the secretion of various enzymes the proteolyze JAMs and other adhesion molecule. B. Extravasation of metastatic cancer cells through transcellular route by creating pores in EC to penetrate the BBB through.

1.2.2. *Toxoplasma Gondii* translocation into the brain:

Toxoplasma gondii (*T. gondii*) is an obligate intracellular parasitic protozoan that infects a broad range of hosts including ~1/3 of the world's population (Figueiredo et al., 2022). According to the statistics of the disease's prevalence and mortality in the United States, the Center for Disease and Prevention (CDC) reported the parasitic infection as neglected, requiring public health action (Ben-Harari & Connolly, 2019).

The parasite life cycle has an asexual stage in humans and other warm-blooded animals and exhibits three infectious stages with distinct morphology: tachyzoites,

bradyzoites and sporozoites (Daher et al., 2021). The latter, the sporozoites, are forms of the parasite that are found in oocysts in felines or cats' feces, as well as in contaminated water or food. Oral ingestion is one route of transmission of *T. gondii* to humans (Daher et al., 2021; Elsheikha et al., 2021). Another way for the human infection is the consumption of contaminated raw or undercooked meat that has tissue cysts (Daher et al., 2021; Elsheikha et al., 2021). Moreover, the parasitic infection is also acquired through transplacental spread of tachyzoites from the infected pregnant mother to her fetus that could lead to abortion or cognition and sight abnormalities in the infant (Bannoura et al., 2018; Singh, 2016). (see Figure 4)

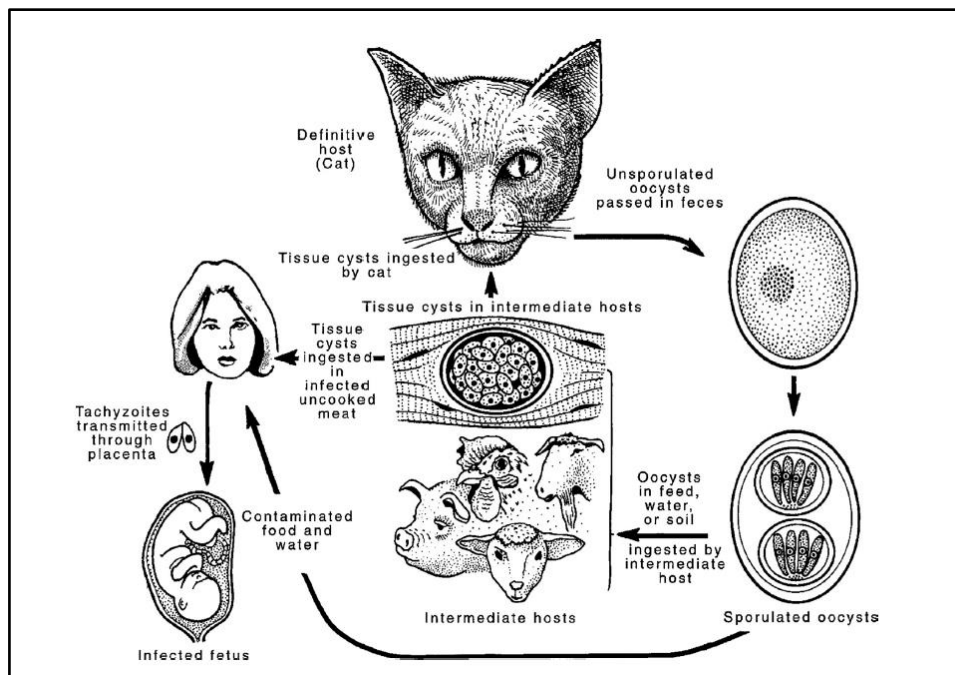


Figure 4: Modalities of infection (Hill & Dubey, 2016).

1.2.2.1. Toxoplasmosis:

The infection with *T. gondii* is called toxoplasmosis and according to different factors, whether the parasite's stage or the host's immunity, it possesses different types. Namely, transplacental infection from a primo-infected pregnant woman to her fetus is

one type and is known as congenital toxoplasmosis (Ramchandrar et al., 2020). Ocular toxoplasmosis is a major cause of blindness and is due to acquired congenital toxoplasmosis that is reactivated by inflammation at the retina (Sauer et al., 2013). Another more quiescent type is acute toxoplasmosis that is known as asymptomatic but can manifest flu-like symptoms in immunocompetent patients, and it is a result of the spread and replication of tachyzoites (Reza Yazdani et al., 2018). When tachyzoites disseminate to the brain, and the host immune system is triggered due to weakening, whether by diseases like HIV or by therapies like chemotherapy or immunosuppressants, the tachyzoites switch to bradyzoites and form cysts in the brain and muscle parenchyma, hence resulting in what is known as chronic toxoplasmosis (Matta et al., 2021). Although bradyzoites do not replicate as fast as tachyzoites, their replication is harmful especially in the brain parenchyma where they affect the neurons, disrupt their connections, and trigger a brain-specific immune response (Daher et al., 2021; Matta et al., 2021). Yet, direct symptoms are still not clearly reported.

1.2.2.2. Associated diseases:

Numerous studies show that *T. gondii* is also associated with multiple primary neuropathies and behavioral disorders. Various research is conducted to investigate the correlation between epilepsy and toxoplasmosis, and results have shown that cryptogenic epilepsy (~20% of epilepsy) recorded a significant increase of *T. gondii* IgG antibodies in comparisons to controls and other epilepsies (Sadeghi et al., 2019; Yazar et al., 2003). Similarly, seroprevalence of the parasite have been significantly higher in Alzheimer's patients as to control groups (Wyman et al., 2017). Moreover, studies have shown that infected humans may manifest behavioral disorders like depression, suicidal attempts,

and schizophrenia, and that is mainly due to altered dopamine levels (Sadeghi et al., 2019; Wang et al., 2015; Wyman et al., 2017).

1.2.2.3. Current treatments:

Current treatments are limited to general anti-bacterial/antiparasitic drugs such as the synergistic combination of pyrimethamine (dihydrofolate reductase (DHFR) enzyme inhibitor), sulfadiazine (dihydropteroate synthase inhibitor) and administration of folinic acid for the management of harmful side effects such as allergy reactions (Ben-Harari et al., 2017). These treatments, whether given prophylactically or therapeutically (vaccines or drugs), do not act upon all three stages of *T. gondii*, and only target the acute phase without having any effect on the chronic phase (Konstantinovic et al., 2019; Montazeri et al., 2017).

1.2.2.4. Imiquimod and its analogues:

Imiquimod is an immunomodulatory drug with antiproliferative, antiparasitic and antiviral activity (Jabari et al., 2019). Imiquimod can activate the innate immune response through MyD88 signaling pathway by binding to the transmembrane protein Toll-like receptor 7 (TLR-7) expressed on monocytes, macrophages, and dendritic cells (DC) (Patra et al., 2018; Sauder, 2000). Following the infection with *T. gondii*, TLRs of DC recognize the parasite through pathogen associated molecular pattern (PAMP) known as profilin (Tashima, 2020; Wu et al., 2017). This activates several signaling pathways initially through MyD88 adaptor protein and also involving mitogen-activated protein kinase (MAPK), leading to the abundant production of multiple immune mediators including interleukin-12 (IL-12), interferon-gamma (INF- γ) and others (Miranda-

Verastegui et al., 2009). Several studies are conducted to assess the potency of imiquimod against toxoplasmosis. Results have shown that treatment with Imiquimod upregulated the expression of TLR-7 leading to cytokine production (Hajj et al., 2021). Moreover, during AT, a reduction in the number of cysts was observed upon CT establishments, and the remaining ones fail to acquire a new infection (Hamie et al., 2021). In addition, the investigation of the drug's efficacy against CT have shown a sharp drop in the number of brain cysts and delayed reactivation and lessen the burden of associated diseases (Hamie et al., 2021). However, Imiquimod is correlated to many side effects including swelling, redness, itching, burning, pain, or clear fluid leakage (Lafaille et al., 2014). Therefore, to tackle these problems, analogues with improved bioavailability are being developed.

1.2.2.5. Modes of *T. gondii* dissemination to the brain:

T. gondii dissemination to the CNS is still not thoroughly studied. Like small lipophilic molecules, it was implied that tachyzoites could transmigrate through the paracellular route by interacting with Tjs (Weight et al., 2015). In the transcellular route, invasion of the parasite was followed by intracellular replication in EC and then basolateral exit to migrate across the basement membrane (Konradt et al., 2016). An alternative and most recently suggested route is called the 'Trojan horse' and is characterised by the hijacking or infection of monocytes/dendritic cells where the infection was reported to increase the host migratory phenotype, transmigratory capability and enhanced adhesion to the endothelium monolayer by integrin-dependent fashion (Ross et al., 2021; Sangaré et al., 2019). However, the trafficking and entry of *T. gondii* to the CNS, the stage of the infection, and whether it disrupts the BBB restrictive permeability or not, remain unresolved. (see Figure 4)

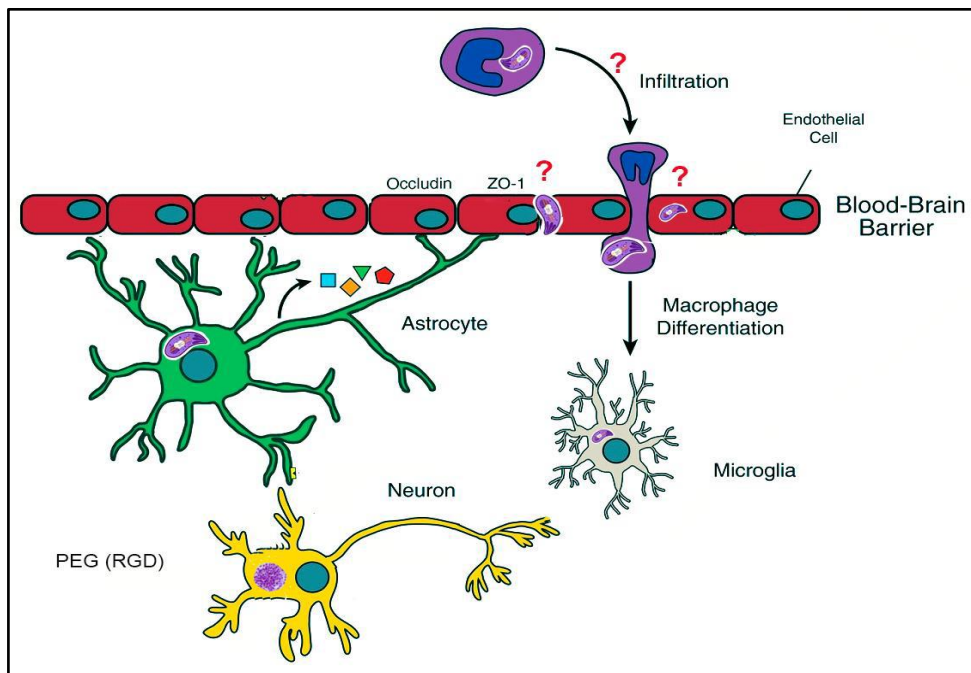


Figure 5: Scenarios of modes of entry of *T. gondii* into the brain.

Therefore, a non-invasive in vitro modelling of the BBB is required to build a platform facilitating the study of the invasion of cancer cells and translocation of parasites and for the screening of current and novel drugs that are permeable to the brain.

1.3. In vitro models that mimic the blood brain barrier:

In vivo animal models are the first models to pave the way for studies regarding the blood brain barrier (Wiranowska et al., 1988). These models demonstrate clear insights on BBB due to their physiological relevance since they include all the structural bases of the BBB and illustrate the effects of the blood flow and biochemical mediators on its function (Hajal et al., 2021). However, in vivo BBB models are not easily accessible due to their complexity and critical localization that makes it difficult to isolate without causing damage to its surroundings whether structurally or functionally (Tietz & Engelhardt, 2015). Moreover, the convoluted interactions of the brain's cellular

compartments complicate the recognition of specific interactions and pathways and their contribution in BBB function (Ogunshola, 2011). In addition, most in vivo animal models failed to translate their findings to human patients where >80% clinical trials of drugs, validated in animals, fail due to genetic, molecular and immunological differences between human and animal BBB (Hajal et al., 2018). Therefore, these limitations with the circulating ethical concerns and high costs have encouraged the search and initiation of alternative in vitro BBB models.

As previously mentioned, to analyse the permeability of the blood brain barrier in health and disease and evaluate drug delivery patterns across the BBB, in vitro models were deemed essential (Achyuta et al., 2013; Fu et al., 2021). These models could be significantly different in their designs, but they usually have a common principle: culturing of endothelial cells on extracellular matrix (ECM) or gels that act as ‘artificial’ (or mimic) ECM on a semipermeable membrane that is in the middle of two liquid compartments demonstrating the luminal and abluminal sides of the barrier and a surrounding complementary microenvironment that is introduced by the coculturing of different cells that are present at the NVU like astrocytes (Modarres et al., 2018; Muruganandam et al., 2002; Nakagawa et al., 2009; Watson et al., 2013). The difference in the developed models include the use of different cell types such as immortalized cell lines, primary cells, and recently several types of stem cells (like embryonic, mesenchymal, neural, induced pluripotent...) (Sivandzade & Cucullo, 2018). Moreover, there was an increase in complexity of the models starting with monocultures to 2D, 3D and dynamic cocultures to furthermore serve a better mimic of the BBB (Cecchelli et al., 2007). (see Table 1)

Up to date, trans-well coculture assay is the most widely used in vitro assay due to its simplicity, minimal requirements and platform that enables the measurement of the membrane's tightness, integrity, and permeability by various techniques like the uptake of dextran, transepithelial electrical resistance (TEER). This assay allows the quantification of genes involved in the barrier tightness (Sivandzade & Cucullo, 2018) and also serves as a platform to study the invasion of different cells and molecules (Stone et al., 2019).

Table 1: Different models of the blood brain barrier (Ferro et al., 2020; Saliba et al., 2018; Sivandzade & Cucullo, 2018; Stone et al., 2019)

In vitro BBB models	Components	Advantages	Disadvantages
Petri dish	Static monoculture of one cell type (mainly EC)	<ul style="list-style-type: none"> ○ very low cost ○ quite simple fabrication ○ easy microscopical visualization of cells ○ ability to assess cell cytotoxicity 	<ul style="list-style-type: none"> ○ unfeasible study of molecular transportation ○ No shear stress
Trans-wells	2D coculture of monolayer EC on a semipermeable membrane and other cell types on either side	<ul style="list-style-type: none"> ○ low cost ○ simple fabrication ○ ability to study drug transportation and invasion assays ○ ideal for linear kinetic studies 	<ul style="list-style-type: none"> ○ no shear stress ○ low TEER (permeability of polar molecules)
Spheroid	3D coculture of one and more cell types (EC, astrocytes...) using gel	<ul style="list-style-type: none"> ○ moderate cost ○ no scaffold ○ ability to study drug transportation and invasion assays 	<ul style="list-style-type: none"> ○ require technical skills ○ not able to measure permeability
Dynamic	3D coculture of monolayer EC on the luminal side of hollow fiber and other cell types on the other side of the membrane	<ul style="list-style-type: none"> ○ moderate cost ○ shear stress ○ ability to study drug transportation and invasion assays ○ high TEER ○ high restricted permeability 	<ul style="list-style-type: none"> ○ time consuming ○ require technical skills ○ need big cellular load ○ not able to visualize the intraluminal compartment
Organ-on-chip	3D coculture of monolayer EC and other cell types in microfluidic channels fabricated using soft lithography techniques	<ul style="list-style-type: none"> ○ high cost ○ realistic dimensions and geometrics ○ expose endothelium to physiological fluid flow ○ allow cells' visualization microscopically 	<ul style="list-style-type: none"> ○ requires technical skills ○ lack of standardized parameters and quantification of critical experimental factors (luminal shear stress, TEER, permeability) ○ not ideal for linear kinetic studies
Microfluidics via 3D printing	3D coculture of monolayer EC and other cell types in microfluidic channels fabricated digitally	<ul style="list-style-type: none"> ○ high cost ○ moderate fabrication ○ require low cell load ○ shear stress ○ allow cells visualization microscopically 	<ul style="list-style-type: none"> ○ require technical skills ○ not ideal for linear kinetic studies

CHAPTER 2

AIMS & OBJECTIVE OF THE STUDY

The attempt to develop in vitro models of the BBB is not a novel approach ranging from 2D monolayers to more complex and sophisticated 3D spheroids and microfluidics. However, several difficulties and pitfalls hinder proper assembly and assessment of model fabrication. Therefore, our general objective is to implicate multicellular primary human cells in our trans-well BBB model that incorporated human endothelial cells and astrocytes that are comparable to in vivo conditions in order to investigate the mechanisms of invasion and drug permeability to the brain.

Specific aim 1: Development of a 3D trans-well BBB model using primary human cells: human aortic endothelial cells and normal human astrocytes.

Specific aim 2: Elucidation of the mechanisms of extravasation of metastatic breast cancer cells to the brain.

Specific aim 3: Illumination of the modes of dissemination of *T. gondii* through the BBB.

CHAPTER 3

MATERIALS AND METHODS

3.1. Cell lines and culture conditions

3.1.1. ECV-304 cell line:

Epithelial cells derived from human umbilical veins exhibit both endothelial and epithelial characteristics. They present many features of endothelial cells and are used as a model for the study of endothelial functions including cell-cell adhesions, angiogenesis and signal transductions (Xiong & Simon, 2011). These cells were purchased from American Type Culture Collection (ATCC) and cultured in Roswell Park Memorial Institute-1640 (RPMI-1640) (Sigma- Aldrich Life Science, Catalog # FBS-HI-12A, Germany), supplemented with 10% fetal bovine serum (FBS) (Capricorn Scientific, Germany), 1% penicillin/streptomycin (Biowest, p/s solution 100x, Catalog # L0022-100), and maintained in a humidified incubator (37°C, 5% CO₂). The cells were passaged at 70-80% confluency using trypsin-EDTA (Sigma-Aldrich Life Science, Catalog# T4549, Germany).

3.1.2. Human Aortic Endothelial Cells (HAEC):

HAECs are endothelial cells isolated from the human aorta and are preferably used in comparison to ECV-304 cell line in our BBB model due to maintaining the morphological and functional characteristics of endothelial cells. Cells cryopreserved at passage 1 with 500,000 cells in each vial were purchased from Lonza, Switzerland Cryopreserved vials containing 500,000 cells at passage one were purchased from Lonza, Switzerland. These cells were cultured in endothelial cells basal medium (iXCells Biotechnology, Catalog#

MD-0010B, USA) supplemented with endothelial cell growth supplement (iXCells Biotechnology, Catalog# MD-0010S, USA) maintained in a humidified incubator (37°C, 5% CO₂). The cells were passaged at 70-80% confluency using trypsin-EDTA (Sigma-Aldrich Life Science, Catalog# T4549, Germany). All subsequent experiments were performed with these cells at passages 5 through 7.

3.1.3. Normal Human Astrocytes (NHA):

NHA are normal human astrocytes isolated from human brain (cerebral cortex) and are used in the BBB modelling as they play a major role in the cytoarchitecture and function of this barrier. Cells are cryopreserved at passage 2 with 500,000 cells in each vial and are purchased from IXCells Biotechnology, USA. These cells were cultured in astrocyte basal medium (iXCells Biotechnology, Catalog# MD-0039B, USA) supplemented with astrocyte growth supplement (iXCells Biotechnology, Catalog# MD-0039S, USA), fetal bovine serum (iXCells Biotechnology, Catalog# MD-0094, USA), and antibiotic-antimycotic (100X) (iXCells Biotechnology, Catalog# MD-0095, USA), and maintained in a humidified incubator (37°C, 5% CO₂). During subculture, flasks were precoated with poly-L-lysine (10% PLL) (Sigma, Missouri, USA) as per manufacturer's recommendations. The cells were passaged at 70-80% confluency using trypsin-EDTA (Sigma-Aldrich Life Science, Catalog# T4549, Germany). All subsequent experiments were performed with these cells at passages 6 through 9.

3.1.4. MDA-MB231 cell line:

Epithelial cells derived from a 51-year-old Caucasian female with metastatic mammary adenocarcinoma 1 (Triple Negative Breast Cancer) and are one of the most used breast cancer cell lines. This cell line displays representative epithelial to mesenchymal transition (EMT) associated with BC metastasis. Therefore, MDA-MB231 cell line was used for the molecular study of BC cell invasion through the BBB as they metastasize to the brain. These cells were purchased from American Type Culture Collection (ATCC) and cultured in RPMI-1640 (Sigma- Aldrich Life Science, Catalog # FBS-HI-12A, Germany), supplemented with 10% fetal bovine serum (FBS) (Capricorn Scientific, Germany), 1% penicillin/streptomycin (Biowest, p/s solution 100x, Catalog # L0022-100), and maintained in a humidified incubator (37°C, 5% CO₂). The cells were passaged at 70-80% confluency using trypsin-EDTA (Sigma-Aldrich Life Science, Catalog# T4549, Germany).

3.1.4.1. MDA-MB 231 shCx 43 cell line:

Cx 43 was silenced using shCx 43 construct (OriGene Technologies, Inc.) (see Figure 6). Transfection of MDA-MB231 cells with shCx 43 construct was previously performed using Lipofectamine 2000 reagent (Invitrogen) according to manufacturer's instructions. Transfected cells were selected in RPMI-1640 (Sigma- Aldrich Life Science, Catalog # FBS-HI-12A, Germany), supplemented with 10% fetal bovine serum (FBS) (Capricorn Scientific, Germany), 1% penicillin/streptomycin (Biowest, p/s solution 100x, Catalog # L0022-100) and puromycin (1 µg/ml). Maintenance medium (RPMI-1640, 10% FBS, 1% P/S with 0.1 µg/ml puromycin) was used throughout the study after cells were selected.

The cells were passaged at 70-80% confluency using trypsin-EDTA (Sigma-Aldrich Life Science, Catalog# T4549, Germany).

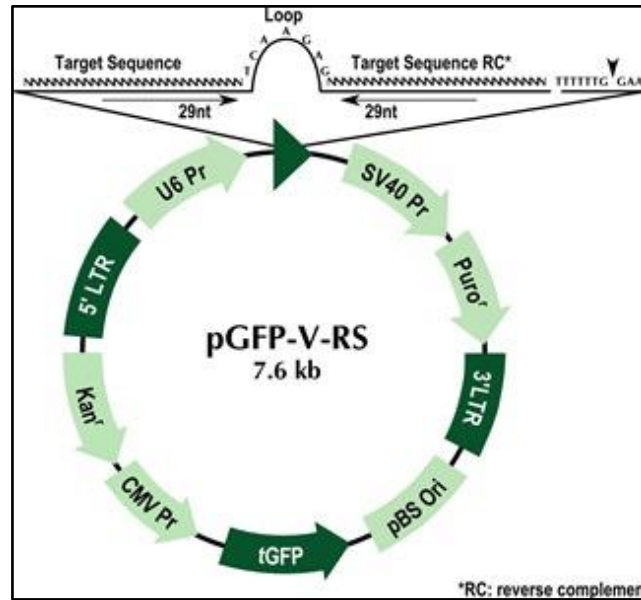


Figure 6: pGFP-V-RS vector used to transfect MDA-MB231 by shCx 43(GFP: green fluorescent protein).

3.2. Cell viability and growth assay

All cell lines were assessed daily using Zen software with a Zeiss Vert A1 microscope (Carl Zeiss AG, Germany) following up on any morphological changes and qualitative proliferation rates. Cells were seeded in 24-well plates at each lines' specific seeding density (see Table 2). At 24, 48, and 72 hours (h), ECV-304, MDA-MB231 and MDA-MB321 shCx 43 cell lines were washed with PBS and trypsinized, whereas NHA and HAEC cells were split at the intended time point.

Table 2: Seeding density of different cell lines per cm²

Cell line	Seeding density per cm ²
ECV-304	20,000
MDA-MB 321/ MDA-MB 321 shCx 43	20,000
HAEC	11,000
NHA	6,000

3.3. BBB modeling:

We developed a three-dimensional (3D) model using a trans-well. 12-well transparent PET membrane cell culture inserts with 0.4 µm pore size (Corning®, USA) were chosen for the initial set-up as they provided the most stable barrier resistance and gave the best cell-cell contact. These inserts were used for barrier integrity assessment (TEER, permeability assay and immunofluorescence). During protocol development, inserts were coated with different dilutions of Matrigel (70-200 µl/cm²) (Corning®, North Carolina, USA). We found that ECV-304 cells formed best monolayer atop of membranes coated with 10% Matrigel, with highest TEER values, suggesting adequate barrier formation.

3.3.1. Coculture of HAEC and NHA:

The need for human primary cells was critical to create a closer representation of the in vivo BBB. Briefly, 12 trans-well inserts (0.4 µm, 10.5 mm) were coated at the apical side with 10% Matrigel and left in the incubator to gel. After 3 hrs, a group of the inserts were seeded with a suspension of NHA (10×10^3 cells) in astrocyte media and 100% Matrigel (1:1), and the other group inserts were seeded with NHA (10×10^3 cells) resuspended in astrocyte media and 10 % Matrigel. Matrigel solidification was attained

after 4 h of incubation at 37°C. This was followed by coating of 10% Matrigel on top of the obtained membrane with embedded NHA. Once embedded cells reached high confluency (~70-80 %), media from the apical side was removed and HAEC were seeded atop (11 × 10³ cells) in endothelial basal media and were left to adhere.

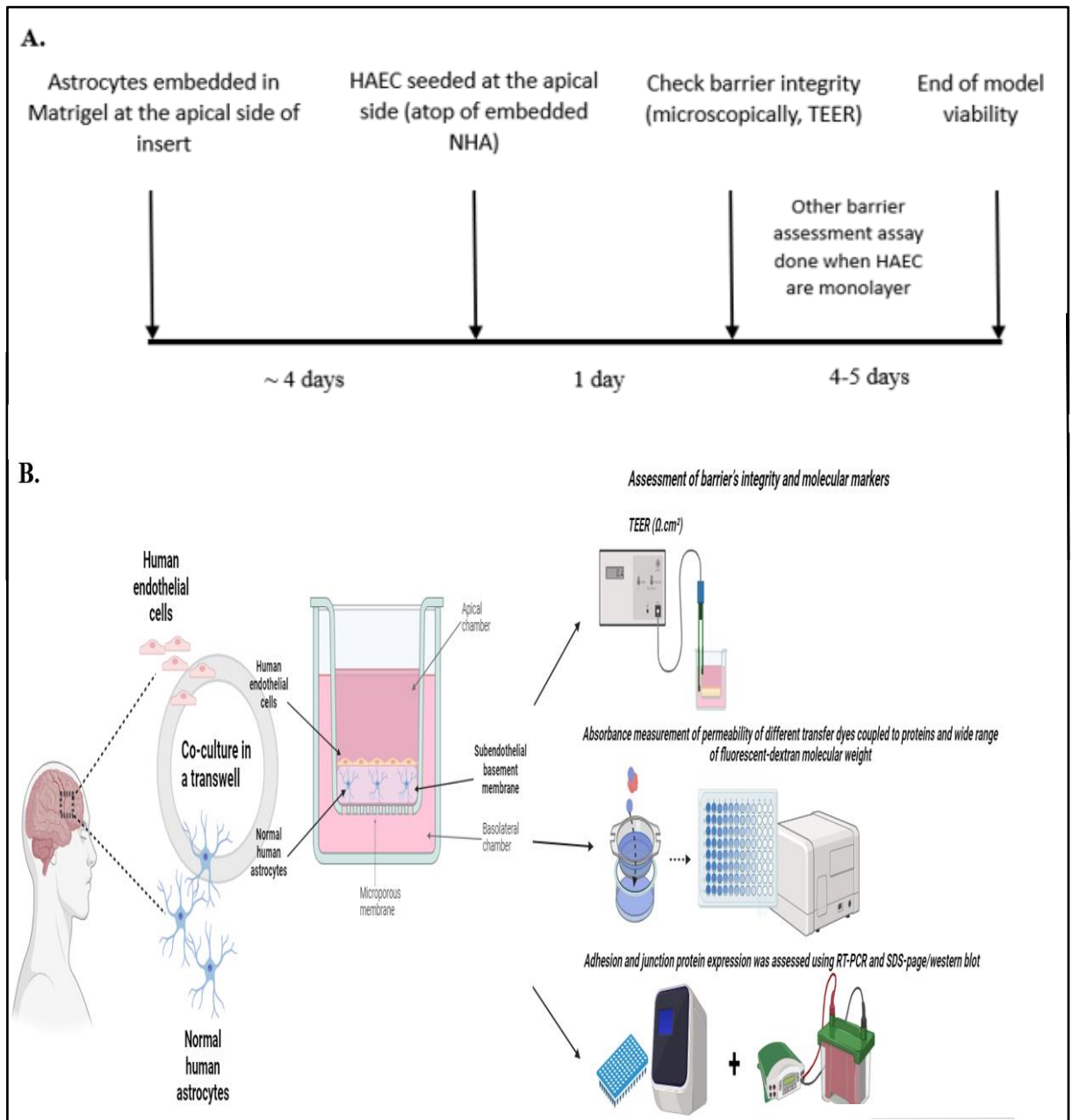


Figure 7: A. Timeline of the stages of model establishment B. HAEC and NHA coculture and further barrier integrity assessment assay done by BioRender.

3.4. Evaluation of the barrier integrity:

3.4.1. *Transepithelial/transendothelial electrical resistance (TEER):*

TEER reflects the flux of ions through the cellular barrier and measures the integrity of endothelial monolayers by describing its impedance. The electrical resistance is expressed as $\Omega \cdot \text{cm}^2$. Briefly, using an EVOM² voltmeter (World Precision Instruments, Florida, USA), STX3 electrodes were first sterilized in 70% ethanol and then placed in phosphate buffer saline (PBS 1X) for 10 mins. The probe was initially equilibrated in a 12-well insert, 0.4 μm -pore size filters/ 0.9 cm^2 growth surface area (Corning®, North Carolina, USA) containing PBS in both compartments. Culture media was removed from all inserts and respective wells, and gently washed twice with PBS. Then, PBS was added 600 μl and 1.6 ml in the apical and basolateral compartments respectively. Readings were repeated 3 times to ensure reproducibility, and the average mean for each insert was subtracted from the blank reading. The result (in Ω) was then multiplied by the growth area (cm^2) of the cell culture inserts.

3.4.2. *Permeability assay:*

3.4.2.1. Evans Blue (EB) and Sodium Fluorescein (NAF) membrane permeability:

EB (961 Da) is a fluorescent marker that strongly binds to proteins in circulation thus its concentration reflects the extravasation of proteins across barriers. NAF (376 Da) is a low molecular weight fluorescent marker that doesn't bind to proteins in circulation and largely depends on its plasma concentration to exudate into the brain. Any perturbation of the barrier integrity will result in seeping of these tracers to the basolateral side. When a confluent endothelial monolayer was observed on the PET transparent 0.4 μm -pore size filter inserts (Corning®, North Carolina, USA), Evans Blue solution (Sigma, Missouri,

USA) was prepared in 1% BSA (67 kDa) (Bovine Serum Albumin, cell culture grade, GIBCO®, Scotland) at a concentration of 170 µg/ml (EB - BSA) and Sodium Fluorescein solution (Sigma, Missouri, USA) was added at a concentration of 10 µg/ml. The solution was then filtered through 0.22 µm-filters (Corning®, Germany). Cells were then washed twice with PBS and 400 µl of solution were added on top of the cells (seeded in inserts). Plate wells were rinsed, and 1.5 ml of PBS was added into each well. Cells were then incubated at 37°C. Every 30 minutes, 200 µl of solution from the well were collected and replaced with fresh 200 µl PBS, for a total of 2 hours. The optical density of the collected solution was measured at 630 nm and 492 nm for Evans Blue and Sodium Fluorescein respectively, and then the concentrations of the markers were calculated.

3.4.2.2. Tetramethyl Rhodamine-Dextran (TRITC-Dextran) membrane permeability:

Dextran is a complex branched polysaccharide made of many glucose molecules falling in a range of 3-2000 kDa molecular weight. These molecules are labelled with biotin, fluorescein isothiocyanate (FITC) or tetramethyl rhodamine (TRITC) to be able to visualize or quantitate their permeability through barriers. TRITC-dextran (10 kDa) (Invitrogen) was prepared in a solution at a concentration of 100 µg/ml and then filtered 0.22 µm-filters (Corning®, Germany). Similarly, as mentioned previously, after washing cells with PBS and adding 1.5 ml PBS to each well, 400 µl of solution were added on top of the cells seeded in inserts. Cells were then incubated at 37°C. Every 30 minutes, 200 µl of solution from the well were collected and replaced with fresh 200 µl PBS, for a total of 2 hours. The optical density of collected solution was recorded at 550 nm, and then concentration of TRITC-dextran was calculated.

3.5. Molecular analysis of junctional proteins expression:

3.5.1. Gene expression assessment by Quantitative Real-Time Polymerase Chain

Reaction:

3.5.1.1. RNA extraction:

Total RNA was extracted from confluent monolayers on inserts of 6-well plates (0.4 μm , 24 mm) (Corning®, USA) using TRI reagent® (Sigma, Germany) as per manufacturer's instructions. Cells were scraped and incubated for 5 mins to be lysed in TRI Reagent® consisting of phenol and guanidine-isothiocyanate. This buffer disrupts the cells, dissolving their cellular components while maintaining RNA integrity due to RNase inhibitor activity. Chloroform was then added to create a non-miscible 3-phase mixture: a colorless upper aqueous colorless layer (containing RNA), an interphase (containing DNA), and a pink lower organic layer (harboring proteins and various cellular contaminants). The aqueous layer was collected, RNA was then precipitated using 100% isopropanol, washed with 75% ethanol. Finally, RNA pellets were resuspended in 20 μl RNase-free water. RNA extracts were quantified by their absorbance at 260 nm and assessed for their purity (260 nm / 280 nm ratio) using a Nanodrop spectrophotometer (DS-11 series spectrophotometer-fluorometer - DeNovix).

3.5.1.2. cDNA synthesis:

2 μg of total RNA extracted was reverse transcribed into complementary DNA (cDNA) using High-Capacity cDNA Reverse Transcription Kits per manufacturer's instructions (appliedbiosystems, Thermofisher).

Quantified RNA samples were added to 2 μl of 10X RT buffer, 0.8 μl of 25X dNTP mix, 2 μl of 10X RT random primers, 1 μl of reverse transcriptase and 4.5 μl of DEPC-treated

water. To allow the annealing of primers to the RNA sequences, samples were incubated at 25°C for 5 minutes followed by the reverse transcription step at 46°C for 20 minutes using a thermal cycler (BioRad T100 thermal cycler, Hercules, CA, USA). The enzymatic activity was terminated by heating the samples at 95°C for 1 minute. The obtained samples were then stored at -80°C until further usage.

3.5.1.3. Quantitative real-time polymerase chain reaction (qRT-PCR):

2µg of cDNA was amplified using a homemade SYBR Green super mix containing dNTPs and Taq DNA polymerase. Samples were loaded in duplicates with the forward and reverse primers specific to each gene in a BioRad CFX96 real-time PCR system. (see Table 3). Cycling conditions were as follows: 95°C for 3 minutes followed by 40 amplification cycles (95°C denaturation for 30 seconds, annealing step for 30 seconds at the primers' annealing temperature, and extension at 72°C for 30 seconds) and a final extension cycle at 72°C for 5 minutes. Relative expression of target genes was assessed by employing the comparative $\Delta\Delta C_t$ method relative to the human glyceraldehyde 3-phosphate dehydrogenase (GAPDH) gene as a normalization reference.

Table 3: RT-qPCR primer sequences and annealing temperatures for studied human

Primers	Oligonucleotide Sequence	Annealing Temperature (°C)
GAPDH	F: TGG TGC TCA GTG TAG CCC AG R: GGA CCT GAC CTG CCG TCT AG	52-62
CLDN 5	F: CTGGACCACAACATCGTGA R: CACCGAGTCGTACACTTTGC	60
ZO-1	F: CAGCCGGTCACGATCTCCT R: TCCGGAGACTGCCATTGC	58
E-cad	F: CAG AAA GTT TTC CAC CAA AG R: AAA TGT GAG CAA TTC TGC TT	58

GAPDH: glyceraldehyde-3-phosphate dehydrogenase/ CLDN 5: claudin 5/ ZO-1: zona occluden 1/ E-cad: epithelial cadherin

3.5.2. Immunofluorescence for phenotypic characterization and adherent junctional protein localization:

Cells were seeded onto 12-well inserts. Subsequently, inserts were divided into 3 conditions: group 1 (endothelial cells (ECV-304 and HAEC) were seeded directly onto insert), group 2 (endothelial cells seeded on inserts coated with 10% Matrigel), and group 3 (coculture where HAEC were seeded atop of NHA embedded in Matrigel (100% or 10%) until a monolayer was observed, after which cells were fixed in 4% paraformaldehyde (PFA) (or cold iced methanol at -20°C). Samples were then permeabilized using 0.1% Triton-X prepared in PBS 1X for 12 minutes and blocked in 5% normal goat serum (NGS) for 1 hour at room temperature (RT). Primary antibodies were prepared in 1% NGS then applied to the inserts for 3 hours at RT. Sample washing was performed using 0.05% Tween in PBS 1X, followed by successive incubations with secondary fluorescent antibodies which were prepared in 1% NGS solution. Another similar washing step as previously mentioned was performed, with a subsequent incubation with 1 µg/µl 4,6-Diamidino-2-Phenylindole, Dihydrochloride (DAPI)

solution staining nuclei. Membranes were cut off from inserts and mounted using an anti-fade mounting solution (Anti-Fade Fluorescence Mounting Medium - Aqueous, Fluoroshield - Abcam) on glass slides then also mounted on the other side with coverslips. Slides were visualized, and images were acquired using Zeiss Axio Observer microscope connected to Zen software and the laser scanning confocal microscope LSM 710 operated by the Zeiss LSM 710 software, Carl Zeiss, Germany.

Table 4: Antibodies used for immunofluorescence.

Antibodies	Manufacturer	Probing
mouse anti-ZO-1	Invitrogen Catalog # 33-9100	Primary antibody
rabbit anti-E-cad	Santa-Cruz Biotechnology Catalog # sc-8987	Primary antibody
mouse anti-GFAP	Abcam Catalog # ab10062	Primary antibody
Alexa Fluor 488 goat anti-mouse	Life Technologies Catalog # A11001	Fluorescent secondary antibody
Alexa Fluor 546 goat anti-mouse	Life Technologies Catalog # A11003	Fluorescent secondary antibody
Texas Red goat anti-rabbit	Invitrogen Molecular Probes Catalog# T2767	Fluorescent secondary antibody

ZO-1: zona occluden 1/ E-cad: epithelial cadherin/ GFAP: glial fibrillary acidic protein

3.6. MDA-MB 231 cells extravasation assay:

Cells were seeded onto 12-well inserts with pore size 8 μm (Corning®, USA). Inserts were divided into 2 groups: group 1 (endothelial cells seeded on inserts coated with 10% Matrigel), and group 2 (coculture of HAEC seeded atop of NHA embedded in 100% Matrigel (1:1)). After an intact monolayer was obtained, each group was subsequently divided into 2 subgroups: first set of inserts had Calcein-AM (Ambeed, USA) stained MDA-MB 231 cells seeded upon the barrier at a high seeding density, and

the second set of inserts had GFP-labeled MDA-MB 231 shCx 43 seeded upon the barrier at a high seeding density. Serum-free RPMI-1640 was added to the upper chamber while RPMI-1640 media supplemented with 10% FBS was added to the lower chamber to ensure chemoattraction. Then, plates were incubated at 37°C for 24 h.

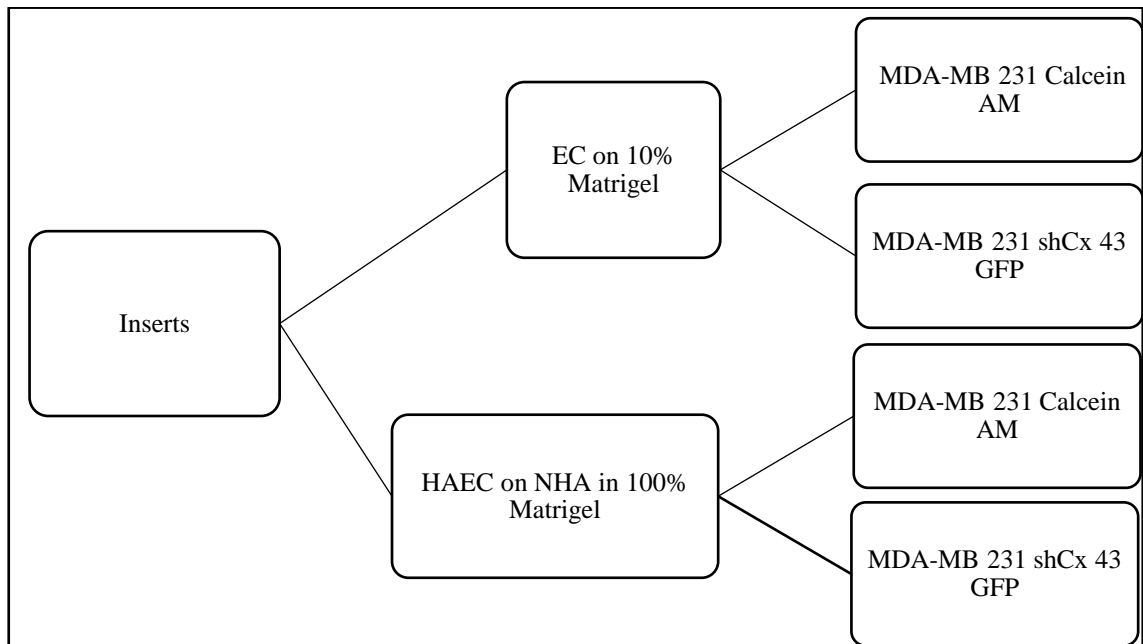


Figure 8: Flow chart of the different insert groups and subsequent division of BC extravasation assay.

3.6.1. Immunofluorescence for migratory BC cells:

To determine the adhesion and migration locations of BCs to EC monolayer, above inserts were removed from their media and gently washed twice with PBS. Subsequently, inserts were incubated with 1 $\mu\text{g}/\mu\text{L}$ 4,6-Diamidino-2-Phenylindole Dihydrochloride (DAPI) solution prepared in 4% PFA, to stain nuclei. Membranes were cut off from inserts and mounted using an anti-fade mounting solution (Anti-Fade Fluorescence Mounting Medium - Aqueous, Fluoroshield - Abcam) on glass slides then also mounted on the other side with coverslips. Slides were visualized and imaged on the laser scanning

confocal microscope LSM 710 operated by the Zeiss LSM 710 software, Carl Zeiss, Germany.

3.7. *T. gondii* invasion assay:

Provided and maintained by Dr. Hiba El-Hajj's lab, GFP- labelled Tachyzoites-II were used throughout this study. Parasites were maintained by serial passage in human foreskin fibroblasts (HFFs) (American Type Culture Collection-CRL 1634), grown in Dulbecco's Modified Eagle's Medium (DMEM) (GIBCO, (Invitrogen) supplemented with 10% of fetal bovine serum (FBS), 1% penicillin–streptomycin, 1% kanamycin and 1% glutamine. THP-1 cells, human monocytes derived from acute leukemia patient, were cultured in DMEM medium supplemented with 10% FBS, 1% sodium pyruvate, 1% penicillin–streptomycin, and 1% glutamine (Invitrogen).

3.7.1. *Parasitic infection of the BBB model:*

Similarly, after an intact monolayer was obtained, each group was subsequently divided into 2 subgroups: first set of inserts had free GFP labelled Tachyzoites introduced to the model at the apical side, and the second set of inserts had THP-1 cells infected with GFP labelled parasites introduced to the BBB model at the apical side of the insert. The parasite/ infected monocytes invasion would be monitored by visualizing the insert after 1, 2 and 4 h using Zen software with a Zeiss Vert A1 microscope (Carl Zeiss AG, Germany).

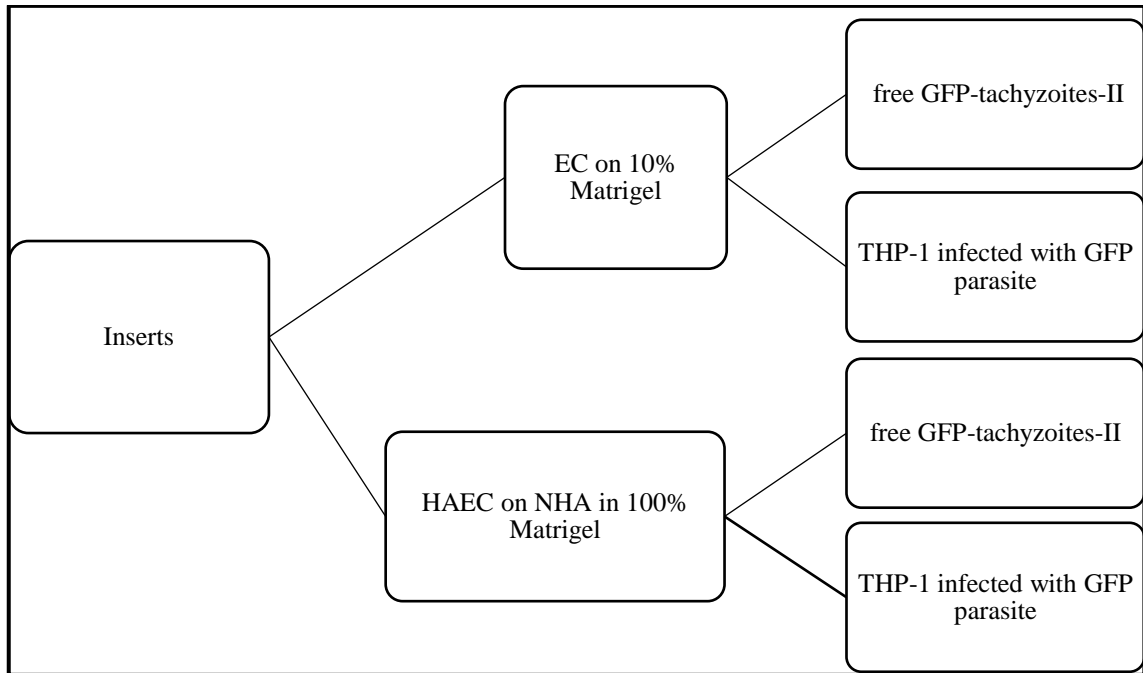


Figure 9: Flow chart of the different insert groups and subsequent division of parasite invasion assay.

3.7.2. *Immunofluorescence for invading parasites/infected monocytes:*

To identify the mode of entry to the brain, cells were incubated at 37°C for 24h to ensure complete invasion. Similarly, inserts were incubated with 1 µg/µL 4,6-Diamidino-2-Phenylindole Dihydrochloride (DAPI) solution in 4% PFA, to stain nuclei. Membranes were cut off from inserts and mounted using an anti-fade mounting solution (Anti-Fade Fluorescence Mounting Medium - Aqueous, Fluoroshield - Abcam) on glass slides then also mounted on the other side with coverslips. Slides were visualized and imaged on the laser scanning confocal microscope LSM 710 operated by the Zeiss LSM 710 software, Carl Zeiss, Germany.

CHAPTER 4

RESULTS

4.1. Endothelial monolayer optimization using ECV-304 cells:

After seeding ECV-304 cells on different dilutions of Matrigel coating, a monolayer was achieved on membranes coated with 20% and 10% Matrigel. Immunofluorescence was performed to localize adhesion junction E-Cad and showed improved expression pattern of this protein in the cells of monolayer seeded atop of 10% Matrigel coating. This was also proved as the expression of the junctional proteins, CLDN 5 and E-Cad, increased in this monolayer. Moreover, highest TEER values were obtained at this monolayer as well. In addition, EB and NaF exhibited the lowest permeability through this monolayer. All the above results indicate that 10% Matrigel coating provides the most suitable conditions to obtain most compact endothelial monolayer.

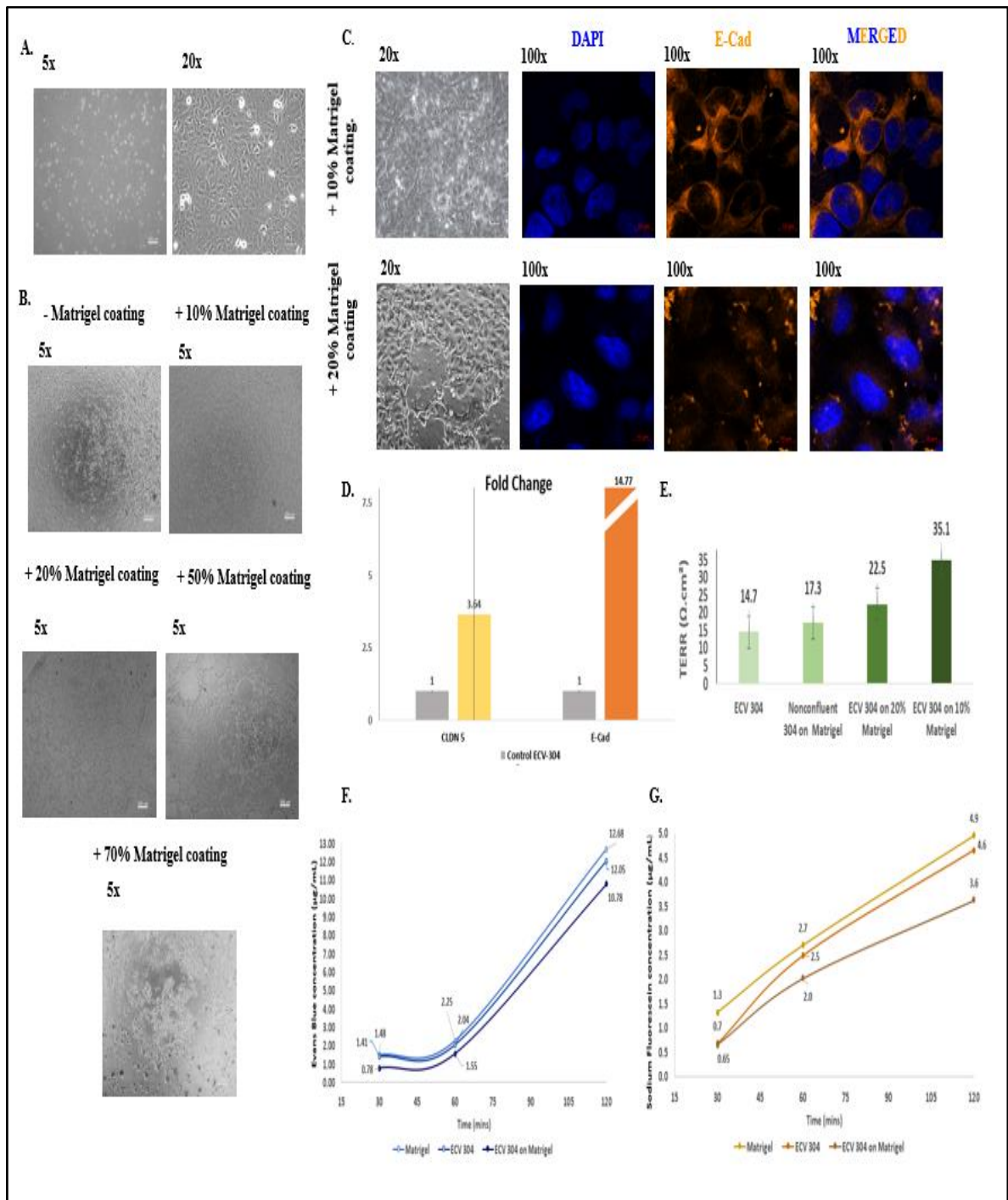


Figure 10: Endothelial monolayer optimization.

(A) Light microscopy images of ECV-304 cells in flask. (B) Light microscopy images of ECV-304 cells seeded on top of coating of different Matrigel dilutions. (C) Immunofluorescence images of ECV-304 cells on 10% and 20% Matrigel coating respectively stained for E-Cad. (D) Bar graphs display the normalized gene expression of CLDN5 and E-Cad in endothelial monolayers on 10% and 20% Matrigel coating as detected by q RT-PCR. (E) Bar graphs indicate average TEER measurements of the previous membrane integrity. Membrane permeability was evaluated by (F) Evans Blue, (G) Sodium Fluorescein permeability assay where levels of molecules that crossed the membrane were measured by spectrophotometry and are plotted as means over time.

4.2. Endothelial monolayer modelling using HAEC:

HAEC were grown as monolayers directly on the apical side of the membrane with/without 10% Matrigel coating. Immunofluorescence was performed to localize adhesion junction ZO-1 and showed improved expression pattern of this protein in the monolayer seeded atop of 10% Matrigel coating. Increased junctional protein expressions, CLDN 5 and ZO-1, in monolayers atop of Matrigel also resulted in a more compact monolayer.

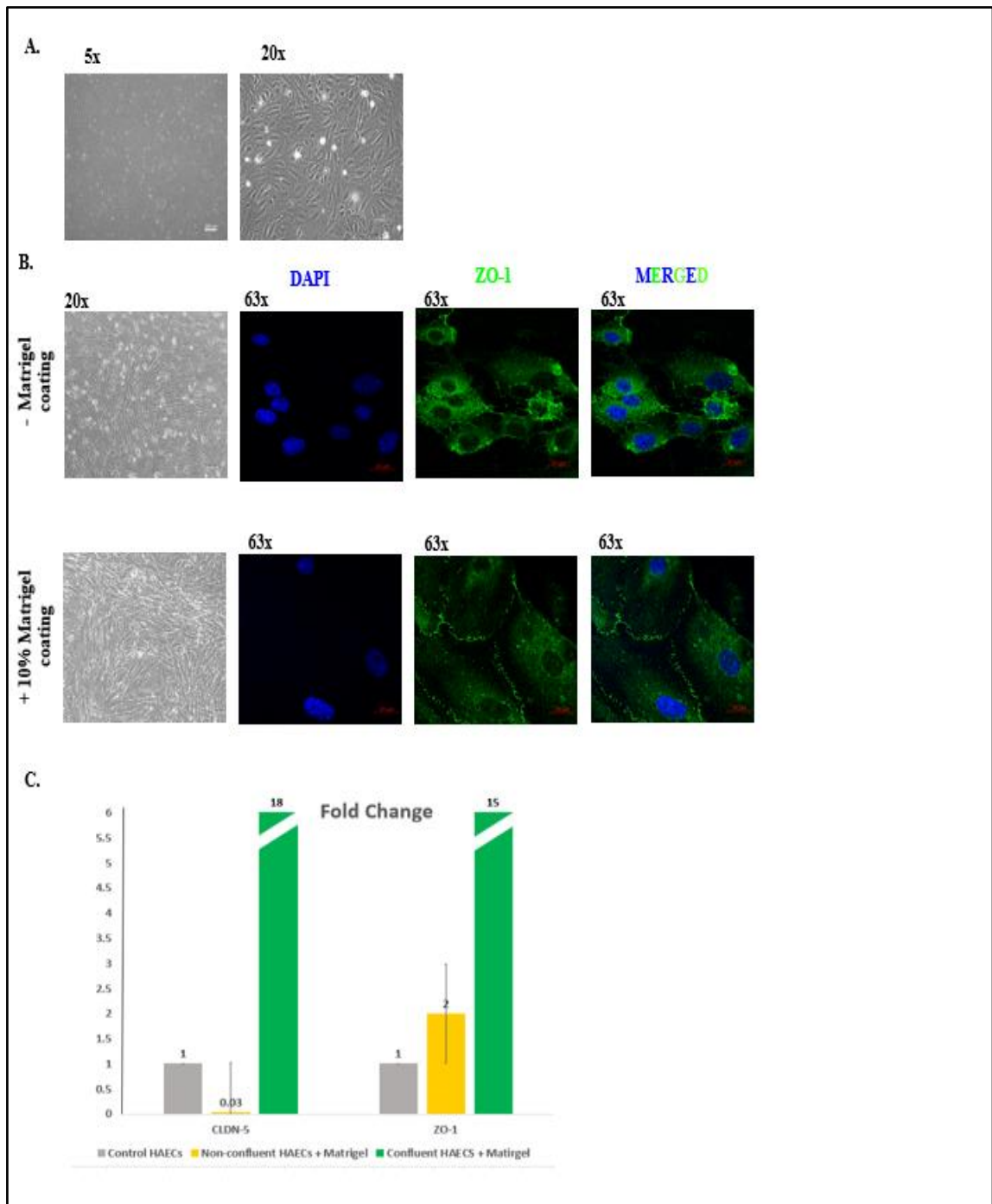


Figure 11: HAEC monolayer characterization.

(A) Light microscopy images of HAEC. (B) Light microscopy and immunofluorescence images for the characterization of HAEC monolayer morphology and junctional adhesion protein pattern staining for ZO-1 in different conditions. (C) Bar graphs display the normalized gene expression of CLDN5 and ZO-1 in endothelial monolayers different conditions as detected by q RT-PCR.

4.3. Normal Human Astrocyte maintenance and 3D culture:

For NHA to have a 3D structure, cells were first embedded in 10% Matrigel and assessed daily for viability and proliferation. At day 14, Calcein-AM staining indicated the viability and increase in number of embedded cells. 50% Matrigel embedment improved 3D structure of the cell highlighted by the GFAP pattern in immunofluorescence images (Fig.12 C) compared to 2D culture (Fig.12 A).

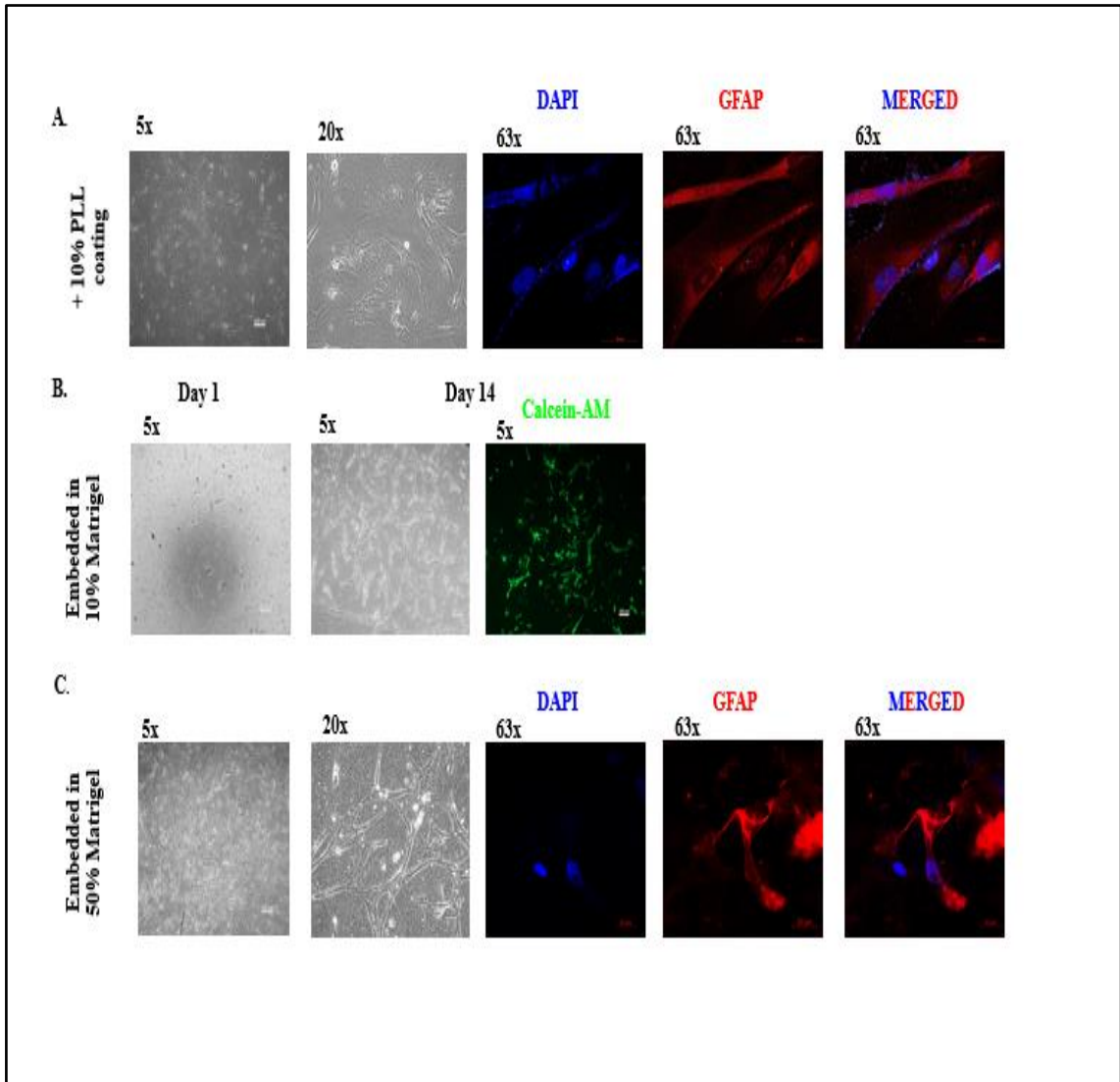


Figure 12: Characterization of NHA morphology, proliferation, and cell viability.

(A) Light microscopy and immunofluorescence images of NHA on PLL coating for morphological characterization by staining for GFAP. (B) Light microscopy to track the proliferation of NHA embedded in 10% Matrigel, and immunofluorescence for Calcein-AM to check cells viability. (C) Light microscopy and immunofluorescence images of NHA embedded in 50% Matrigel for morphological characterization by staining for GFAP.

4.4. BBB modeling using HAEC and NHA:

After seeding HAEC on NHA embedded in 50% Matrigel, a monolayer was achieved. Highest TEER values were obtained for compact monolayer on embedded NHA. In addition, EB, NaF and TRITC-dextran exhibited the lowest permeability through this monolayer. These permeability tests alongside the increased epithelial resistance sets the combination of these cellular components as the most suitable representatives of the *in vivo* properties of the BBB.

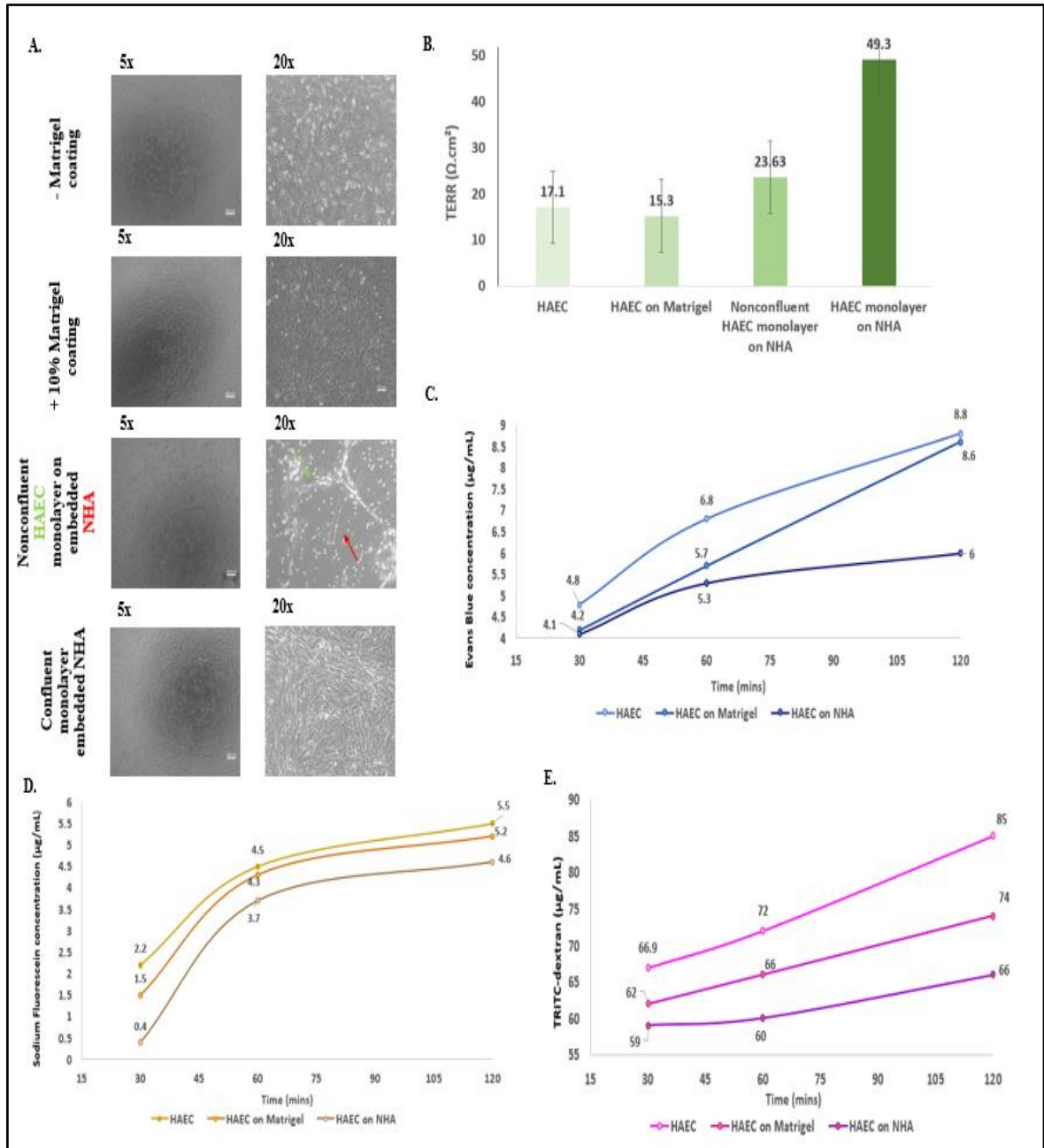


Figure 13: BBB modelling using HAEC and NHA and barrier integrity evaluation.

(A) Light microscopy images of HAEC seeded directly on membrane, on 10% Matrigel coating and on NHA embedded in 50% Matrigel. (B) Bar graphs indicate average TEER measurements of the barrier integrity. Membrane permeability was evaluated by (C) Evans Blue, (D) Sodium Fluorescein and (E) TRITC-dextran permeability assay where levels of molecules crossed the membrane were measured by spectrophotometry and are plotted as means over time.

4.5. MDA-MB231 cell lines successfully extravasate endothelial monolayers:

4.5.1. Extravasation through ECV-304 monolayer:

Calcein-AM stained wild type MDA-MB231 efficiently invaded the monolayer to the basolateral side where they begin to adhere, all while some of the population did not cross the ECV-304 monolayer. However, the downregulation of Cx 43 in shCx 43 MDA-MB 231 cells promotes the invasive capacity of breast cancer cells through the ECV-304 monolayers.

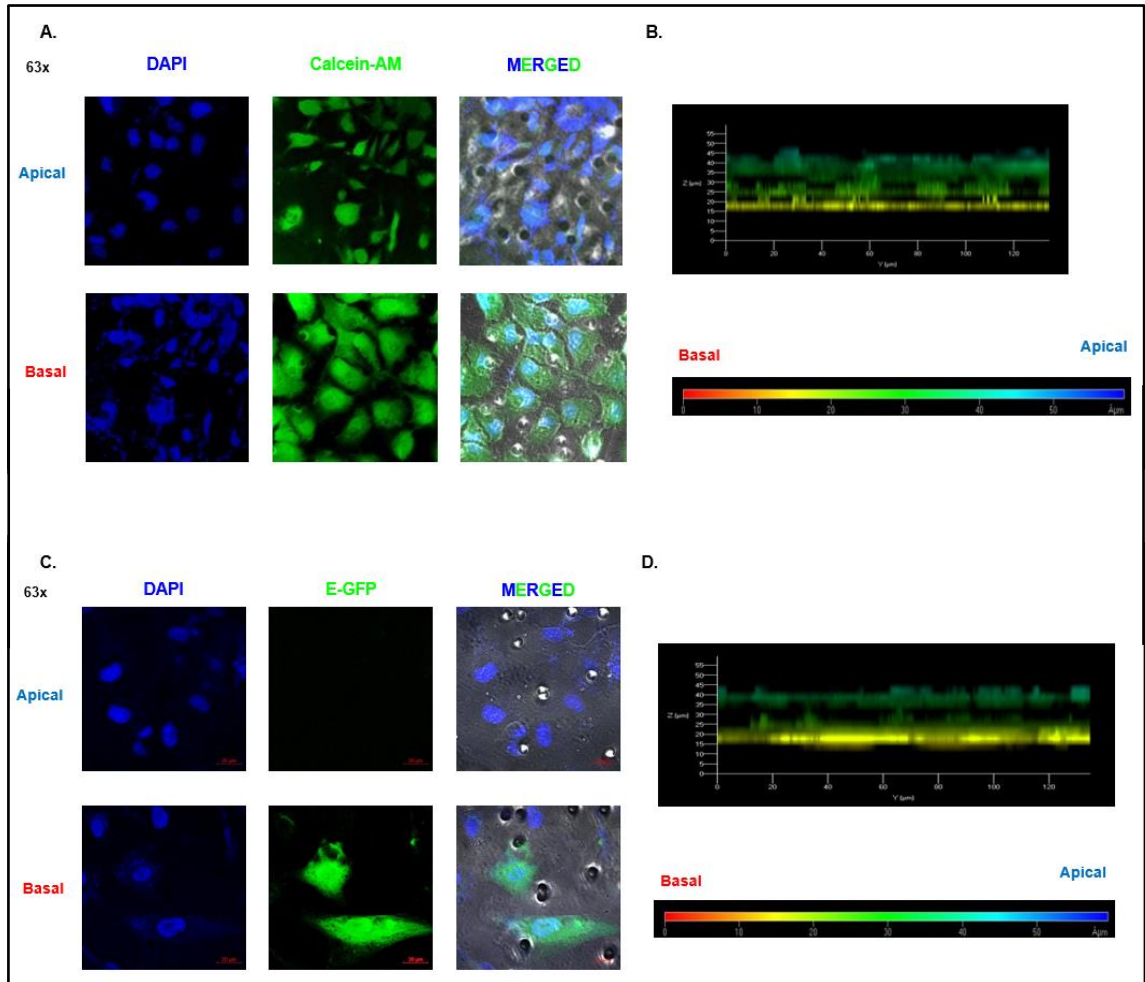


Figure 14: MDA-MB231 cell lines extravasation through ECV-304 monolayer.

(A) z-stack images of extravasating Calcein-AM stained wild type MDA-MB231 cells. (B) 3D gradient presentation of z-stack images of invading wild type MDA-MB231 cells (C) z-stack images of extravasating GFP stained shCx 43 MDA-MB231 cells. (D) 3D gradient presentation of z-stack images of invading shCx 43 MDA-MB231 cells.

4.5.2. Extravasation through HAEC monolayer:

Calcein-AM stained wild type MDA-MB231 efficiently invaded the monolayer to the basolateral side where they begin to adhere, all while some of the population did not cross the ECV-304 monolayer. However, the downregulation of Cx 43 in shCx 43 MDA-MB 231 cells promotes the invasive capacity of breast cancer cells through the ECV-304 monolayers.

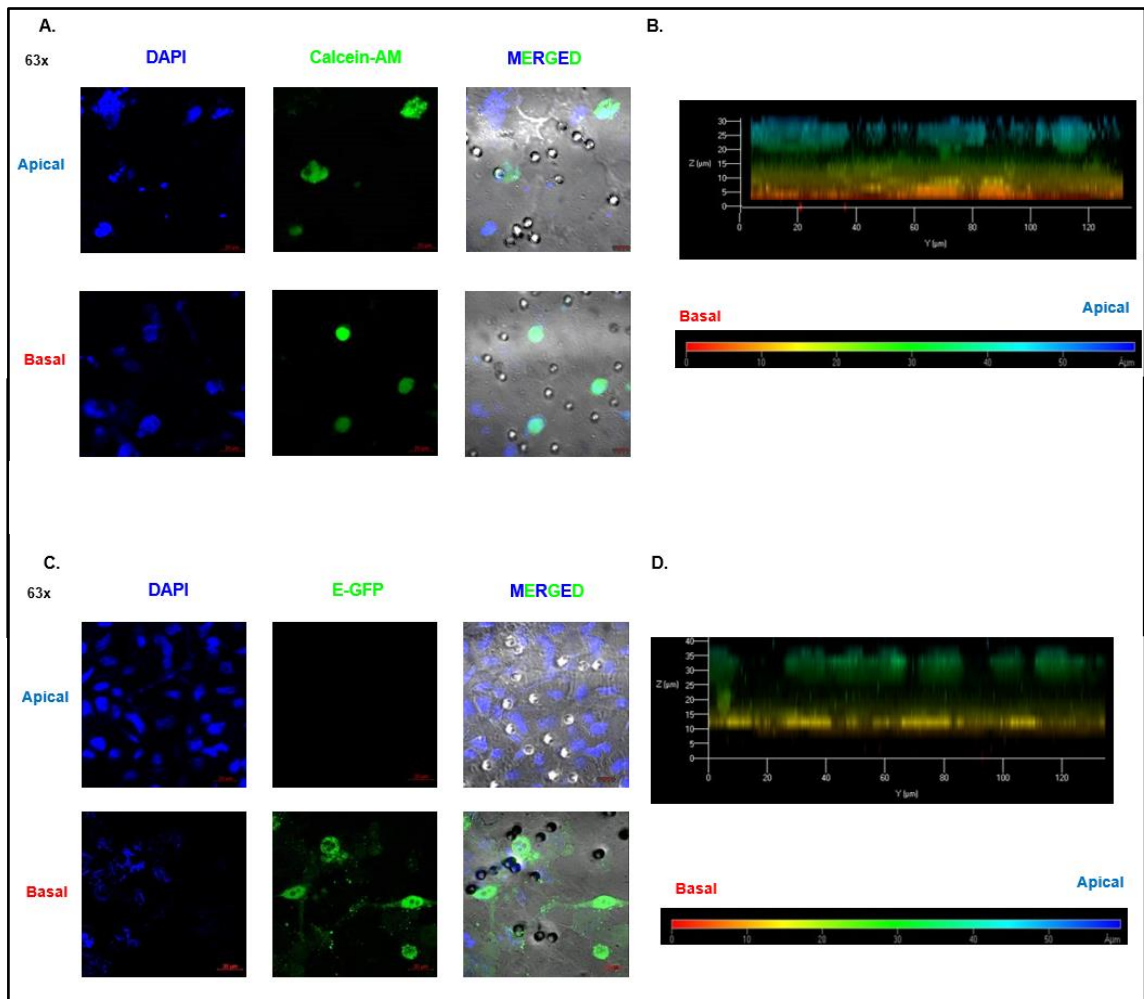


Figure 15: MDA-MB231 cell lines extravasation through HAEC monolayer. (A) z-stack images of extravasating Calcein-AM stained wild type MDA-MB231 cells. (B) 3D gradient presentation of z-stack images of invading wild type MDA-MB231 cells (C) z-stack images of extravasating GFP stained shCx 43 MDA-MB231 cells. (D) 3D gradient presentation of z-stack images of invading shCx 43 MDA-MB231 cells.

4.5.3. Extravasation through HAEC and NHA coculture:

Neither wild type MDA-MB231 nor shCx 43 MDA-MB 231 cells did cross the barrier. This indicates that the barrier we developed is an elite model.

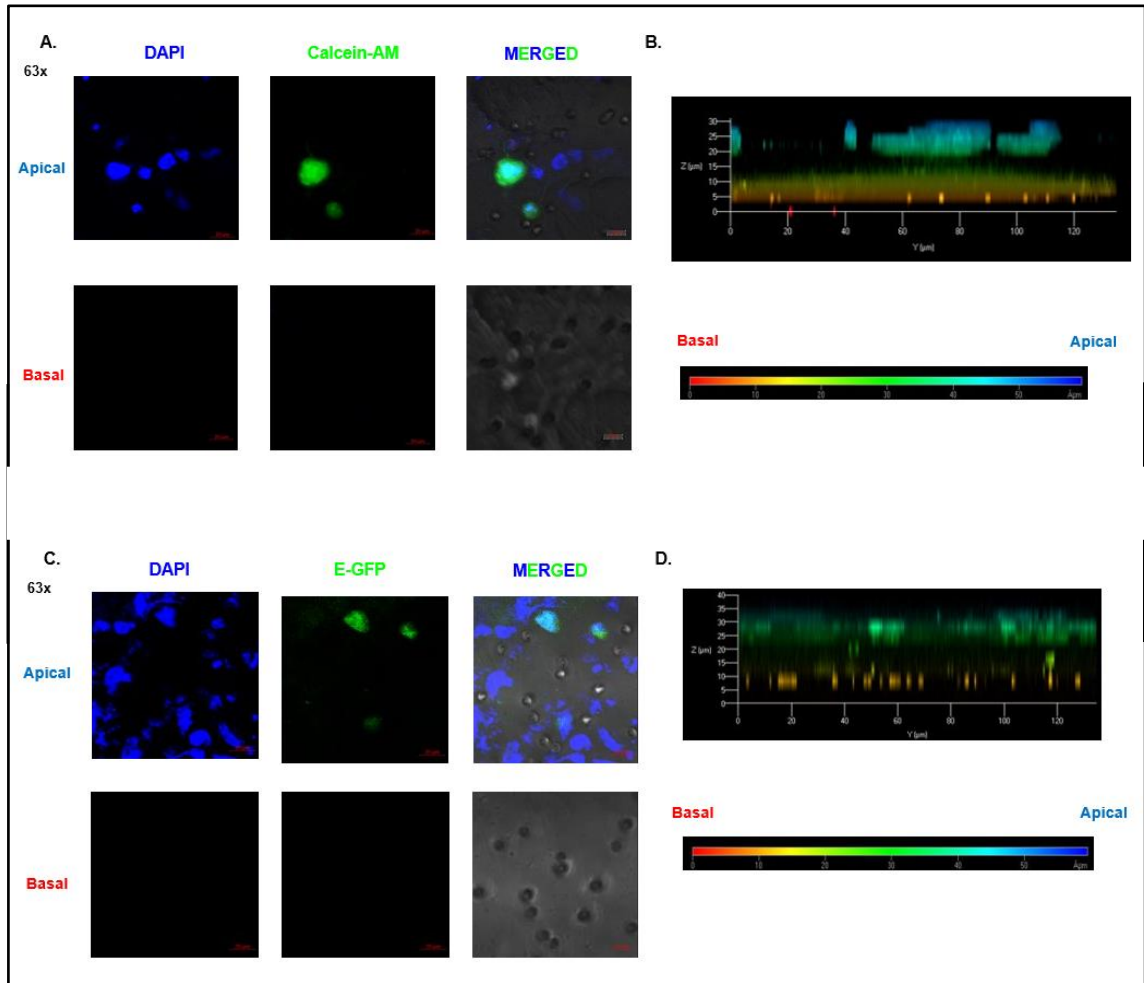


Figure 16: MDA-MB231 cell lines extravasation through HAEC and NHA coculture. (A) z-stack images of extravasating Calcein-AM stained wild type MDA-MB231 cells. (B) 3D gradient presentation of z-stack images of invading wild type MDA-MB231 cells (C) z-stack images of extravasating GFP stained shCx 43 MDA-MB231 cells. (D) 3D gradient presentation of z-stack images of invading shCx 43 MDA-MB231 cells.

4.6. *T. gondii* auspiciously disseminate into endothelial monolayers:

Free GFP- labelled tachyzoite II infect HAEC cells of the endothelial monolayer and reside in its cytoplasm.

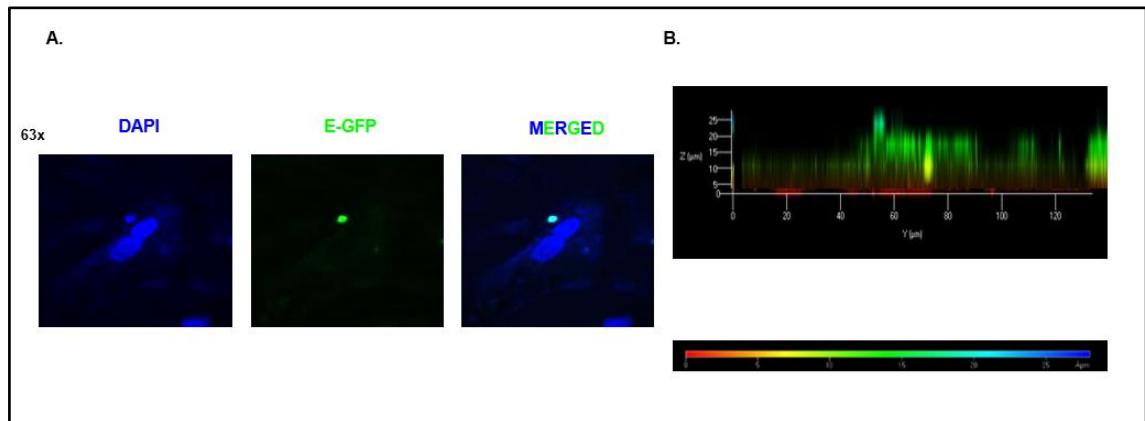


Figure 17: Infection of HAEC cells of the monolayer by GFP labelled tachyzoite II.

CHAPTER 4

DISCUSSION & CONCLUSION

The BBB can be breached in a range of different conditions including cancer metastasis and infections. Research and investigation of these conditions are plagued due the translational difficulties that current in vitro BBB models have. Therefore, our model improves the in vitro translatability of the BBB through uniquely using primary human endothelial cells and astrocytes as well as subendothelial basement membrane to mirror the cyto-architecture of the NVU, to unravel the molecular mechanisms of it being compromised and to assess the permeability of novel drugs delivered to the brain.

We opted to use the trans-well coculture model of the human BBB for our studies owing to incorporate primary astrocytes by embedding them in the subendothelial basement membrane to allow direct interaction with human aortic endothelial monolayer. Our model not only provides a closer resemblance to the BBB, but also is accompanied by high TEER measurements of barrier resistance and low permeability of proteins, solutes, and glucose through the barrier similar to previously published values of other in vitro BBB models (Deli et al., 2005). Moreover, TEER values obtained in the coculture were higher than other trans well models that seeded NHA on the basal side of the insert, thus showing that on the apical side cells have better contact with the endothelial monolayer, hence establishing higher resistance and better integrity (Stone et al., 2019).

The extravasation of wild type metastatic breast cancer cells and downregulated Cx 43 breast cancer cells was assessed through the barrier, and z-stacks of the assay explicitly showed that the downregulation of Cx 43 in these cells promotes for their invasiveness (Kazan et al., 2019). Moreover, the decreased interaction and poor crossing of these cells

through the developed coculture further assure its increasing strength in comparison to endothelial monolayers and other models (Mysiorek et al., 2022).

Using this simple model, we were able to show that the free parasite *T. gondii* can infect HAEC monolayers and stay viable within them (Al-Sandaqchi et al., 2020). Yet, further investigation about its modality of barrier disruption in its free form or hijacking monocytes or T lymphocytes need to be conducted.

However, it is necessary to mention the limitations that we faced during our work. The work was done as one set of experiments; thus, no statistical analysis is performed until further trials. Moreover, limited time for experiments eliminated several steps of imaging and further invasion and drug screening assays. In addition, our model does not incorporate sheer stress and additional cell types present at the NVU that influences cells phenotype and function (Partyka et al., 2017). Therefore, future work should assess these additives into our model.

In summary, the overall function of the BBB is to maintain the brain homeostasis by selectively moderating the exchange of various molecules between the brain parenchyma and the blood flow. During cancer metastasis, inflammation, and parasitic infection, the barriers integrity is disrupted, and consequently other functional and morphological changes occur with in the BBB. Therefor, it is important to fabricate a model of the BBB to study the pathophysiology of cancer and infections, and to screen for novel drugs that target these conditions and their permeability to the brain. We believe our model offers a close presentation of the human BBB while having an easy trans-well set up.

REFERENCES

- Abbott, N. J., Patabendige, A. A., Dolman, D. E., Yusof, S. R., & Begley, D. J. (2010). Structure and function of the blood-brain barrier. *Neurobiol Dis*, 37(1), 13-25. <https://doi.org/10.1016/j.nbd.2009.07.030>
- Abbott, N. J., Rönnbäck, L., & Hansson, E. (2006). Astrocyte–endothelial interactions at the blood–brain barrier. *Nature Reviews Neuroscience*, 7(1), 41-53. <https://doi.org/10.1038/nrn1824>
- Achrol, A. S., Rennert, R. C., Anders, C., Soffiatti, R., Ahluwalia, M. S., Nayak, L., Peters, S., Arvold, N. D., Harsh, G. R., Steeg, P. S., & Chang, S. D. (2019). Brain metastases. *Nat Rev Dis Primers*, 5(1), 5. <https://doi.org/10.1038/s41572-018-0055-y>
- Achyuta, A. K., Conway, A. J., Crouse, R. B., Bannister, E. C., Lee, R. N., Katnik, C. P., Behensky, A. A., Cuevas, J., & Sundaram, S. S. (2013). A modular approach to create a neurovascular unit-on-a-chip. *Lab Chip*, 13(4), 542-553. <https://doi.org/10.1039/c2lc41033h>
- Al-Sandaqchi, A. T., Marsh, V., Williams, H. E. L., Stevenson, C. W., & Elsheikha, H. M. (2020). Structural, Functional, and Metabolic Alterations in Human Cerebrovascular Endothelial Cells during *Toxoplasma gondii* Infection and Amelioration by Verapamil In Vitro. *Microorganisms*, 8(9). <https://doi.org/10.3390/microorganisms8091386>
- Alahmari, A. (2021). Blood-Brain Barrier Overview: Structural and Functional Correlation. *Neural Plast*, 2021, 6564585. <https://doi.org/10.1155/2021/6564585>
- Alyautdin, R., Khalin, I., Nafeeza, M. I., Haron, M. H., & Kuznetsov, D. (2014). Nanoscale drug delivery systems and the blood-brain barrier. *Int J Nanomedicine*, 9, 795-811. <https://doi.org/10.2147/ijn.S52236>
- Armulik, A., Genové, G., Mäe, M., Nisancioglu, M. H., Wallgard, E., Niaudet, C., He, L., Norlin, J., Lindblom, P., Strittmatter, K., Johansson, B. R., & Betsholtz, C. (2010). Pericytes regulate the blood-brain barrier. *Nature*, 468(7323), 557-561. <https://doi.org/10.1038/nature09522>
- Arvanitis, C. D., Ferraro, G. B., & Jain, R. K. (2020). The blood-brain barrier and blood-tumour barrier in brain tumours and metastases. *Nat Rev Cancer*, 20(1), 26-41. <https://doi.org/10.1038/s41568-019-0205-x>
- Baeten, K. M., & Akassoglou, K. (2011). Extracellular matrix and matrix receptors in blood-brain barrier formation and stroke. *Dev Neurobiol*, 71(11), 1018-1039. <https://doi.org/10.1002/dneu.20954>
- Banks, W. A. (2009). Characteristics of compounds that cross the blood-brain barrier. *BMC Neurol*, 9 Suppl 1(Suppl 1), S3. <https://doi.org/10.1186/1471-2377-9-s1-s3>
- Bannoura, S., El Hajj, R., Khalifeh, I., & El Hajj, H. (2018). Acute disseminated encephalomyelitis and reactivation of cerebral toxoplasmosis in a child: Case report. *IDCases*, 13, e00434. <https://doi.org/10.1016/j.idcr.2018.e00434>
- Barar, J., Rafi, M. A., Pourseif, M. M., & Omid, Y. (2016). Blood-brain barrier transport machineries and targeted therapy of brain diseases. *Bioimpacts*, 6(4), 225-248. <https://doi.org/10.15171/bi.2016.30>
- Bellmann, C., Schreivogel, S., Günther, R., Dabrowski, S., Schumann, M., Wolburg, H., & Blasig, I. E. (2014). Highly conserved cysteines are involved in the

- oligomerization of occludin-redox dependency of the second extracellular loop. *Antioxid Redox Signal*, 20(6), 855-867. <https://doi.org/10.1089/ars.2013.5288>
- Ben-Harari, R. R., & Connolly, M. P. (2019). High burden and low awareness of toxoplasmosis in the United States. *Postgrad Med*, 131(2), 103-108. <https://doi.org/10.1080/00325481.2019.1568792>
- Ben-Harari, R. R., Goodwin, E., & Casoy, J. (2017). Adverse Event Profile of Pyrimethamine-Based Therapy in Toxoplasmosis: A Systematic Review. *Drugs R D*, 17(4), 523-544. <https://doi.org/10.1007/s40268-017-0206-8>
- Bos, P. D., Zhang, X. H., Nadal, C., Shu, W., Gomis, R. R., Nguyen, D. X., Minn, A. J., van de Vijver, M. J., Gerald, W. L., Foekens, J. A., & Massagué, J. (2009). Genes that mediate breast cancer metastasis to the brain. *Nature*, 459(7249), 1005-1009. <https://doi.org/10.1038/nature08021>
- Boulay, A. C., Cisternino, S., & Cohen-Salmon, M. (2016). Immunoregulation at the gliovascular unit in the healthy brain: A focus on Connexin 43. *Brain Behav Immun*, 56, 1-9. <https://doi.org/10.1016/j.bbi.2015.11.017>
- Brown, R. C., Egleton, R. D., & Davis, T. P. (2004). Mannitol opening of the blood-brain barrier: regional variation in the permeability of sucrose, but not 86Rb⁺ or albumin. *Brain Res*, 1014(1-2), 221-227. <https://doi.org/10.1016/j.brainres.2004.04.034>
- Brufsky, A. M., Mayer, M., Rugo, H. S., Kaufman, P. A., Tan-Chiu, E., Tripathy, D., Tudor, I. C., Wang, L. I., Brammer, M. G., Shing, M., Yood, M. U., & Yardley, D. A. (2011). Central nervous system metastases in patients with HER2-positive metastatic breast cancer: incidence, treatment, and survival in patients from registHER. *Clin Cancer Res*, 17(14), 4834-4843. <https://doi.org/10.1158/1078-0432.Ccr-10-2962>
- Cash, A., & Theus, M. H. (2020). Mechanisms of Blood-Brain Barrier Dysfunction in Traumatic Brain Injury. *Int J Mol Sci*, 21(9). <https://doi.org/10.3390/ijms21093344>
- Cecchelli, R., Berezowski, V., Lundquist, S., Culot, M., Renftel, M., Dehouck, M. P., & Fenart, L. (2007). Modelling of the blood-brain barrier in drug discovery and development. *Nat Rev Drug Discov*, 6(8), 650-661. <https://doi.org/10.1038/nrd2368>
- Clark, A. G., & Vignjevic, D. M. (2015). Modes of cancer cell invasion and the role of the microenvironment. *Curr Opin Cell Biol*, 36, 13-22. <https://doi.org/10.1016/j.ceb.2015.06.004>
- Coureuil, M., Lécuyer, H., Bourdoulous, S., & Nassif, X. (2017). A journey into the brain: insight into how bacterial pathogens cross blood-brain barriers. *Nat Rev Microbiol*, 15(3), 149-159. <https://doi.org/10.1038/nrmicro.2016.178>
- Cucullo, L., Hossain, M., Puvenna, V., Marchi, N., & Janigro, D. (2011). The role of shear stress in Blood-Brain Barrier endothelial physiology. *BMC Neurosci*, 12, 40. <https://doi.org/10.1186/1471-2202-12-40>
- Daher, D., Shaghlil, A., Sobh, E., Hamie, M., Hassan, M. E., Moumneh, M. B., Itani, S., El Hajj, R., Tawk, L., El Sabban, M., & El Hajj, H. (2021). Comprehensive Overview of Toxoplasma gondii-Induced and Associated Diseases. *Pathogens*, 10(11). <https://doi.org/10.3390/pathogens10111351>
- Daneman, R., & Prat, A. (2015). The blood-brain barrier. *Cold Spring Harb Perspect Biol*, 7(1), a020412. <https://doi.org/10.1101/cshperspect.a020412>

- Deli, M. A., Abrahám, C. S., Kataoka, Y., & Niwa, M. (2005). Permeability studies on in vitro blood-brain barrier models: physiology, pathology, and pharmacology. *Cell Mol Neurobiol*, 25(1), 59-127. <https://doi.org/10.1007/s10571-004-1377-8>
- Duan, S., Luo, X., Zeng, H., Zhan, X., & Yuan, C. (2020). SNORA71B promotes breast cancer cells across blood-brain barrier by inducing epithelial-mesenchymal transition. *Breast Cancer*, 27(6), 1072-1081. <https://doi.org/10.1007/s12282-020-01111-1>
- Dulken, B. W., Buckley, M. T., Navarro Negredo, P., Saligrama, N., Cayrol, R., Leeman, D. S., George, B. M., Boutet, S. C., Hebestreit, K., Pluvinaige, J. V., Wyss-Coray, T., Weissman, I. L., Vogel, H., Davis, M. M., & Brunet, A. (2019). Single-cell analysis reveals T cell infiltration in old neurogenic niches. *Nature*, 571(7764), 205-210. <https://doi.org/10.1038/s41586-019-1362-5>
- Elsheikha, H. M., Marra, C. M., & Zhu, X. Q. (2021). Epidemiology, Pathophysiology, Diagnosis, and Management of Cerebral Toxoplasmosis. *Clin Microbiol Rev*, 34(1). <https://doi.org/10.1128/cmr.00115-19>
- Fares, J., Kanojia, D., Rashidi, A., Ulasov, I., & Lesniak, M. S. (2020). Genes that Mediate Metastasis across the Blood-Brain Barrier. *Trends Cancer*, 6(8), 660-676. <https://doi.org/10.1016/j.trecan.2020.04.007>
- Ferro, M. P., Heilshorn, S. C., & Owens, R. M. (2020). Materials for blood brain barrier modeling in vitro. *Mater Sci Eng R Rep*, 140. <https://doi.org/10.1016/j.mser.2019.100522>
- Figueiredo, C. A., Steffen, J., Morton, L., Arumugam, S., Liesenfeld, O., Deli, M. A., Kröger, A., Schüler, T., & Dunay, I. R. (2022). Immune response and pathogen invasion at the choroid plexus in the onset of cerebral toxoplasmosis. *J Neuroinflammation*, 19(1), 17. <https://doi.org/10.1186/s12974-021-02370-1>
- Fokas, E., Engenhardt-Cabillic, R., Daniilidis, K., Rose, F., & An, H. X. (2007). Metastasis: the seed and soil theory gains identity. *Cancer Metastasis Rev*, 26(3-4), 705-715. <https://doi.org/10.1007/s10555-007-9088-5>
- Friedl, P., & Alexander, S. (2011). Cancer invasion and the microenvironment: plasticity and reciprocity. *Cell*, 147(5), 992-1009. <https://doi.org/10.1016/j.cell.2011.11.016>
- Fu, B. M., Zhao, Z., & Zhu, D. (2021). Blood-Brain Barrier (BBB) Permeability and Transport Measurement In Vitro and In Vivo. *Methods Mol Biol*, 2367, 105-122. https://doi.org/10.1007/978-1-0716-0308-0_308
- Galea, I. (2021). The blood-brain barrier in systemic infection and inflammation. *Cell Mol Immunol*, 18(11), 2489-2501. <https://doi.org/10.1038/s41423-021-00757-x>
- Ganesh, K., & Massagué, J. (2021). Targeting metastatic cancer. *Nat Med*, 27(1), 34-44. <https://doi.org/10.1038/s41591-020-01195-4>
- Geng, Y., Yeh, K., Takatani, T., & King, M. R. (2012). Three to Tango: MUC1 as a Ligand for Both E-Selectin and ICAM-1 in the Breast Cancer Metastatic Cascade. *Front Oncol*, 2, 76. <https://doi.org/10.3389/fonc.2012.00076>
- Goldhirsch, A., Winer, E. P., Coates, A. S., Gelber, R. D., Piccart-Gebhart, M., Thürlimann, B., & Senn, H. J. (2013). Personalizing the treatment of women with early breast cancer: highlights of the St Gallen International Expert Consensus on the Primary Therapy of Early Breast Cancer 2013. *Ann Oncol*, 24(9), 2206-2223. <https://doi.org/10.1093/annonc/mdt303>

- Gosselet, F., Loiola, R. A., Roig, A., Rosell, A., & Culot, M. (2021). Central nervous system delivery of molecules across the blood-brain barrier. *Neurochem Int*, *144*, 104952. <https://doi.org/10.1016/j.neuint.2020.104952>
- Günzel, D., & Yu, A. S. (2013). Claudins and the modulation of tight junction permeability. *Physiol Rev*, *93*(2), 525-569. <https://doi.org/10.1152/physrev.00019.2012>
- Hajal, C., Campisi, M., Mattu, C., Chiono, V., & Kamm, R. D. (2018). In vitro models of molecular and nano-particle transport across the blood-brain barrier. *Biomicrofluidics*, *12*(4), 042213. <https://doi.org/10.1063/1.5027118>
- Hajal, C., Le Roi, B., Kamm, R. D., & Maoz, B. M. (2021). Biology and Models of the Blood-Brain Barrier. *Annu Rev Biomed Eng*, *23*, 359-384. <https://doi.org/10.1146/annurev-bioeng-082120-042814>
- Hajj, R. E., Tawk, L., Itani, S., Hamie, M., Ezzeddine, J., El Sabban, M., & El Hajj, H. (2021). Toxoplasmosis: Current and Emerging Parasite Druggable Targets. *Microorganisms*, *9*(12). <https://doi.org/10.3390/microorganisms9122531>
- Halassa, M. M., Fellin, T., Takano, H., Dong, J. H., & Haydon, P. G. (2007). Synaptic islands defined by the territory of a single astrocyte. *J Neurosci*, *27*(24), 6473-6477. <https://doi.org/10.1523/jneurosci.1419-07.2007>
- Hamie, M., Najm, R., Deleuze-Masquefa, C., Bonnet, P. A., Dubremetz, J. F., El Sabban, M., & El Hajj, H. (2021). Imiquimod Targets Toxoplasmosis Through Modulating Host Toll-Like Receptor-MyD88 Signaling. *Front Immunol*, *12*, 629917. <https://doi.org/10.3389/fimmu.2021.629917>
- Hao, Y., Baker, D., & Ten Dijke, P. (2019). TGF- β -Mediated Epithelial-Mesenchymal Transition and Cancer Metastasis. *Int J Mol Sci*, *20*(11). <https://doi.org/10.3390/ijms20112767>
- Hashimoto, Y., Greene, C., Munnich, A., & Campbell, M. (2023). The CLDN5 gene at the blood-brain barrier in health and disease. *Fluids Barriers CNS*, *20*(1), 22. <https://doi.org/10.1186/s12987-023-00424-5>
- Heithoff, B. P., George, K. K., Phares, A. N., Zuidhoek, I. A., Munoz-Ballester, C., & Robel, S. (2021). Astrocytes are necessary for blood-brain barrier maintenance in the adult mouse brain. *Glia*, *69*(2), 436-472. <https://doi.org/10.1002/glia.23908>
- Hill, D. E., & Dubey, J. P. (2016). Toxoplasma gondii as a Parasite in Food: Analysis and Control. *Microbiol Spectr*, *4*(4). <https://doi.org/10.1128/microbiolspec.PFS-0011-2015>
- Jabari, J., Ghaffarifar, F., Horton, J., Dalimi, A., & Sharifi, Z. (2019). Evaluation of Morphine with Imiquimod as Opioid Growth Factor Receptor or Nalmefene as Opioid Blocking Drug on Leishmaniasis Caused by Leishmania major in Vitro. *Iran J Parasitol*, *14*(3), 394-403.
- Jackson, R. J., Meltzer, J. C., Nguyen, H., Commins, C., Bennett, R. E., Hudry, E., & Hyman, B. T. (2022). APOE4 derived from astrocytes leads to blood-brain barrier impairment. *Brain*, *145*(10), 3582-3593. <https://doi.org/10.1093/brain/awab478>
- Jamieson, J. J., Searson, P. C., & Gerecht, S. (2017). Engineering the human blood-brain barrier in vitro. *J Biol Eng*, *11*, 37. <https://doi.org/10.1186/s13036-017-0076-1>

- Jolly, M. K., Ware, K. E., Gilja, S., Somarelli, J. A., & Levine, H. (2017). EMT and MET: necessary or permissive for metastasis? *Mol Oncol*, *11*(7), 755-769. <https://doi.org/10.1002/1878-0261.12083>
- Kadry, H., Noorani, B., & Cucullo, L. (2020). A blood-brain barrier overview on structure, function, impairment, and biomarkers of integrity. *Fluids Barriers CNS*, *17*(1), 69. <https://doi.org/10.1186/s12987-020-00230-3>
- Kang, S. A., Hasan, N., Mann, A. P., Zheng, W., Zhao, L., Morris, L., Zhu, W., Zhao, Y. D., Suh, K. S., Dooley, W. C., Volk, D., Gorenstein, D. G., Cristofanilli, M., Rui, H., & Tanaka, T. (2015). Blocking the adhesion cascade at the premetastatic niche for prevention of breast cancer metastasis. *Mol Ther*, *23*(6), 1044-1054. <https://doi.org/10.1038/mt.2015.45>
- Kazan, J. M., El-Saghir, J., Saliba, J., Shaito, A., Jalaleddine, N., El-Hajjar, L., Al-Ghadban, S., Yehia, L., Zibara, K., & El-Sabban, M. (2019). Cx43 Expression Correlates with Breast Cancer Metastasis in MDA-MB-231 Cells In Vitro, In a Mouse Xenograft Model and in Human Breast Cancer Tissues. *Cancers (Basel)*, *11*(4). <https://doi.org/10.3390/cancers11040460>
- Keep, R. F., Andjelkovic, A. V., Xiang, J., Stamatovic, S. M., Antonetti, D. A., Hua, Y., & Xi, G. (2018). Brain endothelial cell junctions after cerebral hemorrhage: Changes, mechanisms and therapeutic targets. *J Cereb Blood Flow Metab*, *38*(8), 1255-1275. <https://doi.org/10.1177/0271678x18774666>
- Kim, S. S., Harford, J. B., Pirollo, K. F., & Chang, E. H. (2015). Effective treatment of glioblastoma requires crossing the blood-brain barrier and targeting tumors including cancer stem cells: The promise of nanomedicine. *Biochem Biophys Res Commun*, *468*(3), 485-489. <https://doi.org/10.1016/j.bbrc.2015.06.137>
- Kim, Y., Davidson, J. O., Gunn, K. C., Phillips, A. R., Green, C. R., & Gunn, A. J. (2016). Role of Hemichannels in CNS Inflammation and the Inflammasome Pathway. *Adv Protein Chem Struct Biol*, *104*, 1-37. <https://doi.org/10.1016/bs.apcsb.2015.12.001>
- Konradt, C., Ueno, N., Christian, D. A., Delong, J. H., Pritchard, G. H., Herz, J., Bzik, D. J., Koshy, A. A., McGavern, D. B., Lodoen, M. B., & Hunter, C. A. (2016). Endothelial cells are a replicative niche for entry of *Toxoplasma gondii* to the central nervous system. *Nat Microbiol*, *1*, 16001. <https://doi.org/10.1038/nmicrobiol.2016.1>
- Konstantinovic, N., Guegan, H., Stäjner, T., Belaz, S., & Robert-Gangneux, F. (2019). Treatment of toxoplasmosis: Current options and future perspectives. *Food Waterborne Parasitol*, *15*, e00036. <https://doi.org/10.1016/j.fawpar.2019.e00036>
- Lafaille, F., Solassol, I., Enjalbal, C., Bertrand, B., Doulain, P. E., Vappiani, J., Bonnet, P. A., Deleuze-Masquéfa, C., & Bressolle, F. M. (2014). Structural characterization of in vitro metabolites of the new anticancer agent EAPB0503 by liquid chromatography-tandem mass spectrometry. *J Pharm Biomed Anal*, *88*, 429-440. <https://doi.org/10.1016/j.jpba.2013.09.015>
- Lehmann, S., Te Boekhorst, V., Odenthal, J., Bianchi, R., van Helvert, S., Ikenberg, K., Ilina, O., Stoma, S., Xandry, J., Jiang, L., Grenman, R., Rudin, M., & Friedl, P. (2017). Hypoxia Induces a HIF-1-Dependent Transition from Collective-to-Amoeboid Dissemination in Epithelial Cancer Cells. *Curr Biol*, *27*(3), 392-400. <https://doi.org/10.1016/j.cub.2016.11.057>

- Lockman, P. R., Mittapalli, R. K., Taskar, K. S., Rudraraju, V., Gril, B., Bohn, K. A., Adkins, C. E., Roberts, A., Thorsheim, H. R., Gaasch, J. A., Huang, S., Palmieri, D., Steeg, P. S., & Smith, Q. R. (2010). Heterogeneous blood-tumor barrier permeability determines drug efficacy in experimental brain metastases of breast cancer. *Clin Cancer Res*, *16*(23), 5664-5678. <https://doi.org/10.1158/1078-0432.Ccr-10-1564>
- Mäe, M. A., He, L., Nordling, S., Vazquez-Liebanas, E., Nahar, K., Jung, B., Li, X., Tan, B. C., Chin Foo, J., Cazenave-Gassiot, A., Wenk, M. R., Zarb, Y., Lavina, B., Quaggin, S. E., Jeansson, M., Gu, C., Silver, D. L., Vanlandewijck, M., Butcher, E. C., . . . Betsholtz, C. (2021). Single-Cell Analysis of Blood-Brain Barrier Response to Pericyte Loss. *Circ Res*, *128*(4), e46-e62. <https://doi.org/10.1161/circresaha.120.317473>
- Matta, S. K., Rinkenberger, N., Dunay, I. R., & Sibley, L. D. (2021). Toxoplasma gondii infection and its implications within the central nervous system. *Nat Rev Microbiol*, *19*(7), 467-480. <https://doi.org/10.1038/s41579-021-00518-7>
- Michinaga, S., & Koyama, Y. (2021). Pathophysiological Responses and Roles of Astrocytes in Traumatic Brain Injury. *Int J Mol Sci*, *22*(12). <https://doi.org/10.3390/ijms22126418>
- Miranda-Verastegui, C., Tulliano, G., Gyorkos, T. W., Calderon, W., Rahme, E., Ward, B., Cruz, M., Llanos-Cuentas, A., & Matlashewski, G. (2009). First-line therapy for human cutaneous leishmaniasis in Peru using the TLR7 agonist imiquimod in combination with pentavalent antimony. *PLoS Negl Trop Dis*, *3*(7), e491. <https://doi.org/10.1371/journal.pntd.0000491>
- Modarres, H. P., Janmaleki, M., Novin, M., Saliba, J., El-Hajj, F., RezayatiCharan, M., Seyfoori, A., Sadabadi, H., Vandal, M., Nguyen, M. D., Hasan, A., & Sanati-Nezhad, A. (2018). In vitro models and systems for evaluating the dynamics of drug delivery to the healthy and diseased brain. *J Control Release*, *273*, 108-130. <https://doi.org/10.1016/j.jconrel.2018.01.024>
- Montazeri, M., Sharif, M., Sarvi, S., Mehrzadi, S., Ahmadpour, E., & Daryani, A. (2017). A Systematic Review of In vitro and In vivo Activities of Anti-Toxoplasma Drugs and Compounds (2006-2016). *Front Microbiol*, *8*, 25. <https://doi.org/10.3389/fmicb.2017.00025>
- Muruganandam, A., Tanha, J., Narang, S., & Stanimirovic, D. (2002). Selection of phage-displayed llama single-domain antibodies that transmigrate across human blood-brain barrier endothelium. *Faseb j*, *16*(2), 240-242. <https://doi.org/10.1096/fj.01-0343fje>
- Mustafa, D. A. M., Pedrosa, R., Smid, M., van der Weiden, M., de Weerd, V., Nigg, A. L., Berrevoets, C., Zeneyedpour, L., Priego, N., Valiente, M., Luiders, T. M., Debets, R., Martens, J. W. M., Foekens, J. A., Sieuwerts, A. M., & Kros, J. M. (2018). T lymphocytes facilitate brain metastasis of breast cancer by inducing Guanylate-Binding Protein 1 expression. *Acta Neuropathol*, *135*(4), 581-599. <https://doi.org/10.1007/s00401-018-1806-2>
- Mysiorek, C., Dehouck, L., Gosselet, F., & Dehouck, M. P. (2022). An In Vitro Human Blood-Brain Barrier Model to Study Breast Cancer Brain Metastasis. *Methods Mol Biol*, *2492*, 277-288. https://doi.org/10.1007/978-1-0716-2289-6_16
- Nakagawa, S., Deli, M. A., Kawaguchi, H., Shimizudani, T., Shimono, T., Kittel, A., Tanaka, K., & Niwa, M. (2009). A new blood-brain barrier model using primary

- rat brain endothelial cells, pericytes and astrocytes. *Neurochem Int*, 54(3-4), 253-263. <https://doi.org/10.1016/j.neuint.2008.12.002>
- Nowinski, W. L. (2021). Evolution of Human Brain Atlases in Terms of Content, Applications, Functionality, and Availability. *Neuroinformatics*, 19(1), 1-22. <https://doi.org/10.1007/s12021-020-09481-9>
- Ocaña, O. H., Córcoles, R., Fabra, A., Moreno-Bueno, G., Acloque, H., Vega, S., Barrallo-Gimeno, A., Cano, A., & Nieto, M. A. (2012). Metastatic colonization requires the repression of the epithelial-mesenchymal transition inducer Prrx1. *Cancer Cell*, 22(6), 709-724. <https://doi.org/10.1016/j.ccr.2012.10.012>
- Ogunshola, O. O. (2011). In vitro modeling of the blood-brain barrier: simplicity versus complexity. *Curr Pharm Des*, 17(26), 2755-2761. <https://doi.org/10.2174/138161211797440159>
- Olivera, G. C., Ross, E. C., Peuckert, C., & Barragan, A. (2021). Blood-brain barrier-restricted translocation of *Toxoplasma gondii* from cortical capillaries. *Elife*, 10. <https://doi.org/10.7554/eLife.69182>
- Pan, J., Ma, N., Zhong, J., Yu, B., Wan, J., & Zhang, W. (2021). Age-associated changes in microglia and astrocytes ameliorate blood-brain barrier dysfunction. *Mol Ther Nucleic Acids*, 26, 970-986. <https://doi.org/10.1016/j.omtn.2021.08.030>
- Partyka, P. P., Godsey, G. A., Galie, J. R., Kosciuk, M. C., Acharya, N. K., Nagele, R. G., & Galie, P. A. (2017). Mechanical stress regulates transport in a compliant 3D model of the blood-brain barrier. *Biomaterials*, 115, 30-39. <https://doi.org/10.1016/j.biomaterials.2016.11.012>
- Patra, M. C., Kwon, H. K., Batool, M., & Choi, S. (2018). Computational Insight Into the Structural Organization of Full-Length Toll-Like Receptor 4 Dimer in a Model Phospholipid Bilayer. *Front Immunol*, 9, 489. <https://doi.org/10.3389/fimmu.2018.00489>
- Pedrosa, R., Mustafa, D. A., Soffiatti, R., & Kros, J. M. (2018). Breast cancer brain metastasis: molecular mechanisms and directions for treatment. *Neuro Oncol*, 20(11), 1439-1449. <https://doi.org/10.1093/neuonc/ny044>
- Pellerino, A., Internò, V., Mo, F., Franchino, F., Soffiatti, R., & Rudà, R. (2020). Management of Brain and Leptomeningeal Metastases from Breast Cancer. *Int J Mol Sci*, 21(22). <https://doi.org/10.3390/ijms21228534>
- Ramchandrar, N., Pong, A., & Anderson, E. (2020). Identification of disseminated toxoplasmosis by plasma next-generation sequencing in a teenager with rapidly progressive multiorgan failure following haploidentical stem cell transplantation. *Pediatr Blood Cancer*, 67(4), e28205. <https://doi.org/10.1002/pbc.28205>
- Rasmussen, M. K., Mestre, H., & Nedergaard, M. (2022). Fluid transport in the brain. *Physiol Rev*, 102(2), 1025-1151. <https://doi.org/10.1152/physrev.00031.2020>
- Reza Yazdani, M., Mehrabi, Z., Ataei, B., Baradaran Ghahfarokhi, A., Moslemi, R., & Pourahmad, M. (2018). Frequency of sero-positivity in household members of the patients with positive toxoplasma serology. *Rev Esp Quimioter*, 31(6), 506-510.
- Ross, E. C., Olivera, G. C., & Barragan, A. (2022). Early passage of *Toxoplasma gondii* across the blood-brain barrier. *Trends Parasitol*, 38(6), 450-461. <https://doi.org/10.1016/j.pt.2022.02.003>

- Ross, E. C., Ten Hoeve, A. L., & Barragan, A. (2021). Integrin-dependent migratory switches regulate the translocation of Toxoplasma-infected dendritic cells across brain endothelial monolayers. *Cell Mol Life Sci*, 78(12), 5197-5212. <https://doi.org/10.1007/s00018-021-03858-y>
- Rudziak, P., Ellis, C. G., & Kowalewska, P. M. (2019). Role and Molecular Mechanisms of Pericytes in Regulation of Leukocyte Diapedesis in Inflamed Tissues. *Mediators Inflamm*, 2019, 4123605. <https://doi.org/10.1155/2019/4123605>
- Sadeghi, M., Riahi, S. M., Mohammadi, M., Saber, V., Aghamolaie, S., Moghaddam, S. A., Aghaei, S., Javanian, M., Gamble, H. R., & Rostami, A. (2019). An updated meta-analysis of the association between Toxoplasma gondii infection and risk of epilepsy. *Trans R Soc Trop Med Hyg*, 113(8), 453-462. <https://doi.org/10.1093/trstmh/trz025>
- Saliba, J., Daou, A., Damiati, S., Saliba, J., El-Sabban, M., & Mhanna, R. (2018). Development of Microplatforms to Mimic the In Vivo Architecture of CNS and PNS Physiology and Their Diseases. *Genes (Basel)*, 9(6). <https://doi.org/10.3390/genes9060285>
- Sangaré, L. O., Ólafsson, E. B., Wang, Y., Yang, N., Julien, L., Camejo, A., Pesavento, P., Sidik, S. M., Lourido, S., Barragan, A., & Saeij, J. P. J. (2019). In Vivo CRISPR Screen Identifies TgWIP as a Toxoplasma Modulator of Dendritic Cell Migration. *Cell Host Microbe*, 26(4), 478-492.e478. <https://doi.org/10.1016/j.chom.2019.09.008>
- Sauder, D. N. (2000). Immunomodulatory and pharmacologic properties of imiquimod. *J Am Acad Dermatol*, 43(1 Pt 2), S6-11. <https://doi.org/10.1067/mjd.2000.107808>
- Sauer, A., Rochet, E., Lahmar, I., Brunet, J., Sabou, M., Bourcier, T., Candolfi, E., & Pfaff, A. W. (2013). The local immune response to intraocular Toxoplasma re-challenge: less pathology and better parasite control through Treg/Th1/Th2 induction. *Int J Parasitol*, 43(9), 721-728. <https://doi.org/10.1016/j.ijpara.2013.04.004>
- Savagner, P. (2015). Epithelial-mesenchymal transitions: from cell plasticity to concept elasticity. *Curr Top Dev Biol*, 112, 273-300. <https://doi.org/10.1016/bs.ctdb.2014.11.021>
- Singh, S. (2016). Congenital toxoplasmosis: Clinical features, outcomes, treatment, and prevention. *Trop Parasitol*, 6(2), 113-122. <https://doi.org/10.4103/2229-5070.190813>
- Sivandzade, F., & Cucullo, L. (2018). In-vitro blood-brain barrier modeling: A review of modern and fast-advancing technologies. *J Cereb Blood Flow Metab*, 38(10), 1667-1681. <https://doi.org/10.1177/0271678x18788769>
- Soffietti, R., Ahluwalia, M., Lin, N., & Rudà, R. (2020). Management of brain metastases according to molecular subtypes. *Nat Rev Neurol*, 16(10), 557-574. <https://doi.org/10.1038/s41582-020-0391-x>
- Song, J., Zhang, X., Buscher, K., Wang, Y., Wang, H., Di Russo, J., Li, L., Lütke-Enking, S., Zarbock, A., Stadtmann, A., Striewski, P., Wirth, B., Kuzmanov, I., Wiendl, H., Schulte, D., Vestweber, D., & Sorokin, L. (2017). Endothelial Basement Membrane Laminin 511 Contributes to Endothelial Junctional Tightness and Thereby Inhibits Leukocyte Transmigration. *Cell Rep*, 18(5), 1256-1269. <https://doi.org/10.1016/j.celrep.2016.12.092>

- Soto, M. S., Serres, S., Anthony, D. C., & Sibson, N. R. (2014). Functional role of endothelial adhesion molecules in the early stages of brain metastasis. *Neuro Oncol*, 16(4), 540-551. <https://doi.org/10.1093/neuonc/not222>
- Stone, N. L., England, T. J., & O'Sullivan, S. E. (2019). A Novel Transwell Blood Brain Barrier Model Using Primary Human Cells. *Front Cell Neurosci*, 13, 230. <https://doi.org/10.3389/fncel.2019.00230>
- Suhail, Y., Cain, M. P., Vanaja, K., Kurywchak, P. A., Levchenko, A., Kalluri, R., & Kshitiz. (2019). Systems Biology of Cancer Metastasis. *Cell Syst*, 9(2), 109-127. <https://doi.org/10.1016/j.cels.2019.07.003>
- Tashima, T. (2020). Smart Strategies for Therapeutic Agent Delivery into Brain across the Blood-Brain Barrier Using Receptor-Mediated Transcytosis. *Chem Pharm Bull (Tokyo)*, 68(4), 316-325. <https://doi.org/10.1248/cpb.c19-00854>
- Tietz, S., & Engelhardt, B. (2015). Brain barriers: Crosstalk between complex tight junctions and adherens junctions. *J Cell Biol*, 209(4), 493-506. <https://doi.org/10.1083/jcb.201412147>
- Tsai, J. H., & Yang, J. (2013). Epithelial-mesenchymal plasticity in carcinoma metastasis. *Genes Dev*, 27(20), 2192-2206. <https://doi.org/10.1101/gad.225334.113>
- Uemura, M. T., Maki, T., Ihara, M., Lee, V. M. Y., & Trojanowski, J. Q. (2020). Brain Microvascular Pericytes in Vascular Cognitive Impairment and Dementia. *Front Aging Neurosci*, 12, 80. <https://doi.org/10.3389/fnagi.2020.00080>
- Verkman, A. S. (2002). Aquaporin water channels and endothelial cell function. *J Anat*, 200(6), 617-627. <https://doi.org/10.1046/j.1469-7580.2002.00058.x>
- Vranic, S., & Gatalica, Z. (2022). An Update on the Molecular and Clinical Characteristics of Apocrine Carcinoma of the Breast. *Clin Breast Cancer*, 22(4), e576-e585. <https://doi.org/10.1016/j.clbc.2021.12.009>
- Wang, Y., Ye, F., Liang, Y., & Yang, Q. (2021). Breast cancer brain metastasis: insight into molecular mechanisms and therapeutic strategies. *Br J Cancer*, 125(8), 1056-1067. <https://doi.org/10.1038/s41416-021-01424-8>
- Wang, Z. T., Harmon, S., O'Malley, K. L., & Sibley, L. D. (2015). Reassessment of the role of aromatic amino acid hydroxylases and the effect of infection by *Toxoplasma gondii* on host dopamine. *Infect Immun*, 83(3), 1039-1047. <https://doi.org/10.1128/iai.02465-14>
- Watson, P. M., Paterson, J. C., Thom, G., Ginman, U., Lundquist, S., & Webster, C. I. (2013). Modelling the endothelial blood-CNS barriers: a method for the production of robust in vitro models of the rat blood-brain barrier and blood-spinal cord barrier. *BMC Neurosci*, 14, 59. <https://doi.org/10.1186/1471-2202-14-59>
- Weight, C. M., Jones, E. J., Horn, N., Wellner, N., & Carding, S. R. (2015). Elucidating pathways of *Toxoplasma gondii* invasion in the gastrointestinal tract: involvement of the tight junction protein occludin. *Microbes Infect*, 17(10), 698-709. <https://doi.org/10.1016/j.micinf.2015.07.001>
- Wilhelms, D. B., Kirilov, M., Mirrasekhian, E., Eskilsson, A., Kugelberg, U., Klar, C., Ridder, D. A., Herschman, H. R., Schwaninger, M., Blomqvist, A., & Engblom, D. (2014). Deletion of prostaglandin E2 synthesizing enzymes in brain endothelial cells attenuates inflammatory fever. *J Neurosci*, 34(35), 11684-11690. <https://doi.org/10.1523/jneurosci.1838-14.2014>

- Winkler, L., Blasig, R., Breitzkreuz-Korff, O., Berndt, P., Dithmer, S., Helms, H. C., Puchkov, D., Devraj, K., Kaya, M., Qin, Z., Liebner, S., Wolburg, H., Andjelkovic, A. V., Rex, A., Blasig, I. E., & Haseloff, R. F. (2021). Tight junctions in the blood-brain barrier promote edema formation and infarct size in stroke - Ambivalent effects of sealing proteins. *J Cereb Blood Flow Metab*, *41*(1), 132-145. <https://doi.org/10.1177/0271678x20904687>
- Wiranowska, M., Wilson, T. C., Bencze, K. S., & Prockop, L. D. (1988). A mouse model for the study of blood-brain barrier permeability. *J Neurosci Methods*, *26*(2), 105-109. [https://doi.org/10.1016/0165-0270\(88\)90158-6](https://doi.org/10.1016/0165-0270(88)90158-6)
- Wong, A. D., Ye, M., Levy, A. F., Rothstein, J. D., Bergles, D. E., & Searson, P. C. (2013). The blood-brain barrier: an engineering perspective. *Front Neuroeng*, *6*, 7. <https://doi.org/10.3389/fneng.2013.00007>
- Wu, S. K., Chu, P. C., Chai, W. Y., Kang, S. T., Tsai, C. H., Fan, C. H., Yeh, C. K., & Liu, H. L. (2017). Characterization of Different Microbubbles in Assisting Focused Ultrasound-Induced Blood-Brain Barrier Opening. *Sci Rep*, *7*, 46689. <https://doi.org/10.1038/srep46689>
- Wyman, C. P., Gale, S. D., Hedges-Muncy, A., Erickson, L. D., Wilson, E., & Hedges, D. W. (2017). Association between Toxoplasma gondii seropositivity and memory function in nondemented older adults. *Neurobiol Aging*, *53*, 76-82. <https://doi.org/10.1016/j.neurobiolaging.2017.01.018>
- Xiong, W. C., & Simon, S. (2011). ECV304 Cells: An Endothelial or Epithelial Model? *J Biol Chem*, *286*(41), 1e21. <https://doi.org/10.1074/jbc.N111.261073>
- Xu, L., Nirwane, A., & Yao, Y. (2019). Basement membrane and blood-brain barrier. *Stroke Vasc Neurol*, *4*(2), 78-82. <https://doi.org/10.1136/svn-2018-000198>
- Yang, Y., Estrada, E. Y., Thompson, J. F., Liu, W., & Rosenberg, G. A. (2007). Matrix metalloproteinase-mediated disruption of tight junction proteins in cerebral vessels is reversed by synthetic matrix metalloproteinase inhibitor in focal ischemia in rat. *J Cereb Blood Flow Metab*, *27*(4), 697-709. <https://doi.org/10.1038/sj.jcbfm.9600375>
- Yazar, S., Arman, F., Yalçın, S., Demirtaş, F., Yaman, O., & Sahin, I. (2003). Investigation of probable relationship between Toxoplasma gondii and cryptogenic epilepsy. *Seizure*, *12*(2), 107-109. [https://doi.org/10.1016/s1059-1311\(02\)00256-x](https://doi.org/10.1016/s1059-1311(02)00256-x)
- Yurchenco, P. D. (2011). Basement membranes: cell scaffoldings and signaling platforms. *Cold Spring Harb Perspect Biol*, *3*(2). <https://doi.org/10.1101/cshperspect.a004911>
- Zaragozá, R. (2020). Transport of Amino Acids Across the Blood-Brain Barrier. *Front Physiol*, *11*, 973. <https://doi.org/10.3389/fphys.2020.00973>